

Reservoir Characterization by Investigating the Reservoir Fluid Properties and their Effect on Seismic Response of Fenchuganj Gas Field, Bangladesh

SM Ariful Islam¹, Md. Shofiquil Islam^{1*} and Mohammad Moinul Hossain², Md Aminul Islam³

¹Department of Petroleum and Mining Engineering, Shahjalal University of Science and Technology, Sylhet 3114 Bangladesh

²Geophysical Division, Bangladesh Petroleum Exploration and Production Company (BAPEX), Dhaka, Bangladesh

³Department of Petroleum Geoscience, Faculty of Science Universiti Brunei Darussalam Jalan Tungku Link Gadong BE1410, Negara Brunei Darussalam

Abstract

Fenchuganj Gas Field is located in the Surma Basin of Bangladesh and characterized by water-drive gas field. In the reservoir condition, water saturation increases as gas production rise. The fluid properties of the four individual gas zones of this reservoir at the present condition and at the gas depleted condition should be addressed with proper prediction. In this paper, we characterize the total reservoir with special emphasis on Upper Gas Zone and New Gas Zone I which are compared with other two gas zones (New Gas Zone III and New Gas Zone II) representing some modeling results (has done before by these authors) which evidences that the pore fluids have a significant effect on the acoustic impedance and the Poisson's ratio of the reservoir rock which is directly correlated with seismic amplitudes at constant pressure with Batzle-Wang model and Gassman-Boit models. These models with varying pressure and water saturation conditions show the reasonable predicted fluid modulus against pressure for all four gas sands. The reservoir modeling from irreducible water saturation condition (90% gas saturation) to residual gas condition (10% gas saturation) provides a way to estimate values at reservoir conditions from logging conditions. Fluid bulk density increases when water saturation increases with constant pressure and stay around constant when water saturation increases with pressure drop. But overall it increases through the production path that we assumed. Amplitude versus Offset (AVO) analysis is also compared with other study models which show that seismic reflection of p-wave changes due to change of pressure and water saturation of the reservoir rock layers. This study is also showing that all four gas zones of the Fenchuganj are under gas sand category 3. We propose the modeling of fluid property in determining the convenience of time lapse seismic, predicting AVO and amplitude response, and forecasting in the study field and making production and reservoir engineering decisions.

Keywords: Fluid; Reservoir characterization; Gas sand; Saturation; AVO

Introduction

Reservoir characterization incorporates all the characteristics of the reservoir that are relevant to its ability to store hydrocarbons and also to produce them. Models for reservoir characterization are used to suggest the behavior of the fluids within the reservoir under different sets of situation and to find the best possible production techniques that will maximize the production.

However, for the interpretation and evaluation of structural or stratigraphic features in the subsurface, the seismic data are commonly used. The physical properties of pore fluids have a vital effect on the seismic response of a porous rock containing it. It is essential to have an understanding of the changes in p-wave (compressional) velocity, s-wave (shear) velocity, and density as fluid or rock properties change to know or predict the effect of changes in seismic amplitudes and travel times.

For determination of the fluid properties from well log and seismic data, different methods are used (e.g., [1-10]). In this study, we have used Batzle and Wang [8] model, Gassmann [2] -Biot [3] model and AVO (Zoeppritz equation) model. The Batzle and Wang [8] model determines fluid properties, whereas, the Gassmann-Biot model predicts the saturated rock properties in reservoir rock matrix and gives a forecast of future effects of saturated rock properties on seismic response. Moreover, the AVO (amplitude variation with offset) model predicts the seismic response from the layered rock properties [11].

The amplitude versus offset (AVO) is a general term in reflection seismology for referring to the dependency of the seismic attribute, amplitude, with the distance between the source and receiver (the

offset). AVO analysis is a method that geophysicists can accomplish on seismic data to determine a rock's fluid content, porosity, density or seismic velocity, shear wave information, fluid indicators (hydrocarbon indications [12]). The P-wave and S-wave velocity, bulk density, acoustic impedance, Poisson's ratio (PR), and bulk modulus are determined from Batzle and Wang [8] without considering the rock matrix and from Gassmann-Biot models as a function of the saturating rock fluids.

Fenchuganj Gas Field is one of major gas producing fields in the Surma basin with estimated reserves of 553 Bcf. These authors already have worked on first two zones (New gas Zone [13] III and New gas Zone II) of Fenchuganj Gas Field. However, it is required to work with all four layers for better reservoir characterization [31]. Here we aimed i) to predict the velocity, density and modulus of fluid/fluid saturated rock matrix samples for both varying saturation with constant/varying pressure using Batzle and Wang model and Gassmann-Biot model, and ii) to predict seismic response from the layered rock properties using

***Corresponding author:** Md. Shofiquil Islam, Department of Petroleum and Mining Engineering, Shahjalal University of Science and Technology, Sylhet 3114 Bangladesh, Tel. 880821711945; E-mail: sho_fiq@yahoo.com

Received September 27, 2014; **Accepted** November 15, 2014; **Published** November 22, 2014

Citation: Islam SMA, Islam MS, Hossain MM, Islam MA (2014) Reservoir Characterization by Investigating the Reservoir Fluid Properties and their Effect on Seismic Response of Fenchuganj Gas Field, Bangladesh. J Fundam Renewable Energy Appl 4: 144. doi: [10.4172/20904541.1000144](https://doi.org/10.4172/20904541.1000144)

Copyright: © 2014 Islam SMA, et al. This is an open-access article distributed under the terms of the Creative Commons Attribution License, which permits unrestricted use, distribution, and reproduction in any medium, provided the original author and source are credited.

AVO (Zoeppritz equation) for all four layers with special emphasize on Upper Gas Zone (most targeted zone) and New Gas Zone I of Fenchuganj Gas Field.

Geological Setting and Stratigraphy of the Study Area

Fenchuganj structure of Surma basin lies under Fenchuganj Upazila of Sylhet district. It is about forty kilometers southeast of Sylhet town. Geographically, it is bounded by longitude 90°53' - 92° east and latitude 24°30' - 24°37' north and it is tectonically located in the transition zone between the central Surma basin and the Folded Belt in the east (Figure 1).

The Surma Basin of Bangladesh experienced a variety of sediment facies, indicating a range of depositional environments during the Neogene time [15]. Furthermore, during the Miocene time, the Sylhet Basin has a noticeable subsidence and marine transgression. The transgression of the Miocene certainly affected the coastline. It is believed that the Surma Basin has undergone two successive phases of evolution; the marine transgressive phase, followed by a regressive phase resulting in a series of continental fluvio-deltaic to marginal marine sedimentation during the Neogene. The thickness of the late Mesozoic and Cenozoic strata in the Surma Basin range is from about 13 to 17 km [15,16], and much of this group is Neogene in age. The Great Himalayan Orogeny and related tectonics subject the Surma Basin during the Miocene-Pliocene times. However, major changes in sea level for Neogene are transgressive-regressive phenomena suggested by [15].

Fenchuganj structure is an elongated structure and about 30 km long and 8 km wide. It is a reversibly faulted asymmetrical anticline with NNE- SSW trending axis [16]. The eastern flank has sharp dip than the western flank. The amount of dip in the eastern flank varies from 30°-35°, whereas in the western flank dip varies from 20° to 25°.

Fenchuganj anticline is structurally higher in comparison to Jalalabad, KailashTila, and Beanibazar anticline with reference to Upper Marine Shale of Miocene age, but it is lower than Atgram anticline according to prominent horizon like Upper Marine Shale (UMS). The exposed rock is Dupi Tila of Plio-Pleistocene age. The formation of our targeted layers is Bokabil and Bhuban [17].

Methodology

In this paper, we have used Batzle and Wang [8], and Gassmann-Biot [2,3] model for varying/constant saturation with varying/constant pressure condition. We used the input values from well test analysis. The detailed methodology is reported our previous paper [16]. The AVO calculation of Zoeppritz equation was also performed to predict the layer rock property and to compare with aforesaid two methods for better confidence are also described by Islam et al [16].

Result and Discussion

Four gas bearing zones are present and identified in the Fenchuganj gas field. They are New Gas Zone III, New Gas Zone II, Upper Gas Zone and New Gas Zone I. Analysis of all four gas zones is presented in this paper while analysis of the first two gas zones has already published [17]. We emphasized on the mainly Upper Gas Zone and new gas Zone I, and compared the results with other two zones. The results of all zones are tabled of course.

New Gas Zone III was found at a depth of 1656-1680m, with pressure 16.3888 MPa (2377psi), temperature 46.67°C (116°F), porosity 27.3%, gas saturation 54%, water saturation 46% and salinity 8500 ppm. The New Gas Zone II with depth 1992-2017 m, pressure 19.7328 MPa (2862psi), temperature 51.11°C (124°F), porosity 14.5%, gas saturation 36%, water saturation 64% and salinity 9500 ppm. The Upper Gas Zone with depth 2030-2086 m, pressure 20.1121 MPa (2917 psi), temperature 51.67°C (125°F), porosity 25%, gas saturation 60%, water saturation 40% and salinity 10000 ppm. And the New Gas Zone I with depth 2148-2154 m, pressure 21.2841 MPa (3087psi), temperature 55.56°C (132°F), porosity 24.8%, gas saturation 57%, water saturation 43% and salinity 10500 ppm. For all gas zones, density of airs 0.00122g/cc, the API gravity of condensate is 31.86°, gas-condensate ratio is 142260, gas constant(R) is 8.3145, and specific gravity of gas is 0.5624. These are the initial condition of gas layers Table 2. Fluid properties for gas zones were analyzed using the aforementioned methods of the previous paper by these authors [17]. Our main aim was to investigate and forecast the behavior of reservoir fluid properties during production which are discussed below.

Fluid models for Varying Saturation under Constant Pressure

Batzle and Wang Model: Using Batzle and Wang model for varying saturation with constant pressure for initial conditions, i.e. parameters, we have calculated density (ρ), acoustic velocity (V_p) and modulus (k) of gas, brine and mixture phase (Table 3).

The calculated result shows that the density(ρ), acoustic velocity (V_p) and bulk modulus (k) are 0.1367 g/cm³, 3,549.46 m/s, and 41.25 MPa for Upper Gas Zone, whereas New gas Zone I shows these values are 0.1412 g/cm³, 559.70 m/s, and 44.24 MPa, respectively for gas phase (Table 3). For brine and mixture phase, all the parameters (density, acoustic velocity and bulk modulus) have changed significantly (Table 3).

The cross-plot between bulk modulus and density for changing the saturation of gas zones have been formulated which are given in Figure 2. The values of modulus and density for changing saturation are listed in Table 4.

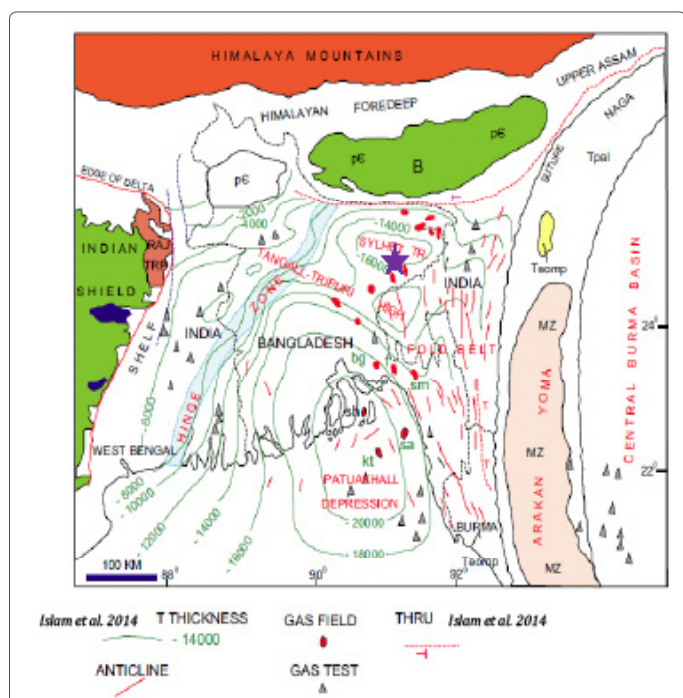


Figure 1: Generalized geological map of Bangladesh and adjoining area. Surma Basin is same as Sylhet Trough (after [14]); the purple asterisk locates the reservoir area.

Age	Formation	Depth (m)	Thickness (m)	Lithology
Recent	Alluvium	0-30	30	Unconsolidated sand, silt and clay
Late Pliocene	DupiTila	30-298	268	Mostly sandstone and minor clay. Sandstone: Brown to light brown, coarsesand
Middle Pliocene	Tipam	298-1150	852	Mostly sandstone and minor clay. Sandstones are light to off white, medium, ferruginous, poorly consolidated, and composed of mainly quartz with few mica & dark color minerals
Miocene	Upper Bokabil	1150-1466	316	Grey to bluish grey shale, soft to moderately hard and compact, and also laminated.
	Middle Bokabil	1466-1766	300	Sandstone and shale alteration
	Lower Bokabil	1766-2236	470	Mostly shale with minor sandstone
Early Miocene	Upper Bhuban	2236- down to 4977	914-2741 (Vary)	Alternation of sandstone and shale, with minor calcareous siltstone

Table 1: Lithostratigraphic succession of Fenchuganj Gas Field (after [15.16]).

Gas Zones	Measured Depth, m	Pressure, MPa	Temperature, °C	Porosity, Φ	Gas Saturation, S _g	Water Saturation, S _w	Salinity, ppm
New Gas Zone III	1656-1680	16.3888	46.67	0.273	0.54	0.46	8500
New Gas Zone II	1992-2017	19.7328	51.11	0.145	0.36	0.64	9500
Upper Gas Zone	2030-2086	20.1121	51.67	0.25	0.6	0.40	10000
New Gas Zone I	2148-2154	21.2841	55.56	0.248	0.57	0.43	10500
Density of Air, ρ _{air} = 0.00122 g/cc at 15.6°C							
°API Gravity of Condensate = 31.86°							
Gas-Condensate ratio = 142260							
Gas Constant, R = 8.3145							
Specific gravity of Gas, G = 0.5624							

Table 2: Input Values for Batzle and Wang Model.

Calculation For New Gas Zone III (Islam et al. 2014)			
Properties	Gas	Brine	Mixture
Density, g/cc	0.1151	1.002	0.523
Acoustic Velocity, m/s	526.3145	1574.348	334.126
Bulk Modulus, Mpa	31.8754	2483.332	58.390
Calculation For New Gas Zone II (Islam et al. 2014)			
Properties	Gas	Brine	Mixture
Density, g/cc	0.1346	1.0022	0.6899
Acoustic Velocity, m/s	546.925	1586.719	397.097
Bulk Modulus, MPa	40.2731	2523.198	108.783
Calculation For Upper Gas Zone			
Properties	Gas	Brine	Mixture
Density, g/cc	0.1367	1.0025	0.4829
Acoustic Speed, m/s	549.464	1588.479	375.295
Bulk Modulus, Mpa	41.2594	2529.461	68.026
Calculation For New Gas Zone I			
Properties	Gas	Brine	Mixture
Density, g/cc	0.141	1.0016	0.511
Acoustic Speed, m/s	559.699	1595.112	387.108
Bulk Modulus, Mpa	44.236	2548.473	76.602

Table 3: Calculated Values for Batzle and Wang Model (for varying saturation with constant pressure).

Saturations of gas zones change from the initial condition with production. In Figure 2, the red marked position is the initial condition, whereas the green line indicates the production direction. These Figures show that for saturation changes with constant pressure, both the bulk modulus and density increases as the water saturation increases. However, the density increases very rapidly and bulk modulus increases slowly at the initial stage of production, whereas reverse situation (density increases slowly and bulk modulus increases very rapidly) exists at the later stage.

Gassmann-Biot model: In this section, Table 5 and Table 6 demonstrate the use of the Gassmann-Biot equations with fluid and rock properties to determine the overall reservoir rock seismic properties such as velocity and density. The input values include porosity (ρ), solid material bulk modulus (K_s) and density (ρ_s), brine

density (ρ_w), bulk modulus (K_w), hydrocarbon density (ρ_{hyd}) and bulk modulus (K_{hyd}). The important output values are the bulk density (ρ_d), P-wave velocity (V_p), S-wave velocity (V_s), acoustic impedance (A_i), and Poisson's ratio (σ) as they vary due to changes in saturation. The dry frame modulus is held constant.

Using the Gassmann-Biot model at the reservoir condition, we found that the values of dry frame rigidity (G) are 6.58438 and 3.83328 GPA, bulk density (ρ) are 2.19998 and 2.1947707 g/cm³, fluid bulk modulus (K_f) are 0.068027 and 0.076594 GPA, saturated bulk modulus (KB) are 34.610512 and 16.74993 GPA, compressional wave velocity (V_p) are 4441.031 and 3118.338 m/s, shear wave velocity (V_s) are 1730.0079 and 1321.572 for Upper Gas Zone and New Gas Zone I, respectively (Table 6). Some other values of output parameters for different saturation are listed in Table 6.

Modulus-Density for Saturation Change							
Gas and Brine (New Gas Zone III) (Islam et al. 2014)				Gas and Brine (New Gas Zone II) (Islam et al. 2014)			
Gas%	Brine%	Density, g/cc	Modulus, Gpa	Gas%	Brine%	Density, g/cc	Modulus, Gpa
5	95	0.958	0.5125	5	95	0.959	0.618
10	90	0.913	0.2857	10	90	0.915	0.3521
20	80	0.825	0.1516	20	80	0.829	0.1893
30	70	0.736	0.1032	30	70	0.742	0.1294
40	60	0.647	0.0782	40	60	0.655	0.0983
50	50	0.558	0.0629	50	50	0.568	0.0793
60	40	0.469	0.0527	60	40	0.482	0.0664
70	30	0.381	0.0453	70	30	0.393	0.0571
80	20	0.292	0.0397	80	20	0.308	0.0501
90	10	0.204	0.0354	90	10	0.221	0.0447
Gas and Brine (Upper Gas Zone)				Gas and Brine (New Gas Zone I)			
Gas%	Brine%	Density, g/cc	Modulus, Gpa	Gas%	Brine%	Density, g/cc	Modulus, Gpa
5	95	0.959	0.6299	5	95	0.959	0.6653
10	90	0.916	0.3598	10	90	0.916	0.3826
20	80	0.829	0.1937	20	80	0.83	0.2068
30	70	0.743	0.1325	30	70	0.743	0.1417
40	60	0.656	0.1007	40	60	0.657	0.1078
50	50	0.569	0.0812	50	50	0.571	0.0869
60	40	0.483	0.0681	60	40	0.485	0.0729
70	30	0.396	0.0585	70	30	0.399	0.0627
80	20	0.309	0.0514	80	20	0.313	0.0551
90	10	0.223	0.0458	90	10	0.229	0.0491

Table 4: Modulus and density for different saturation condition.

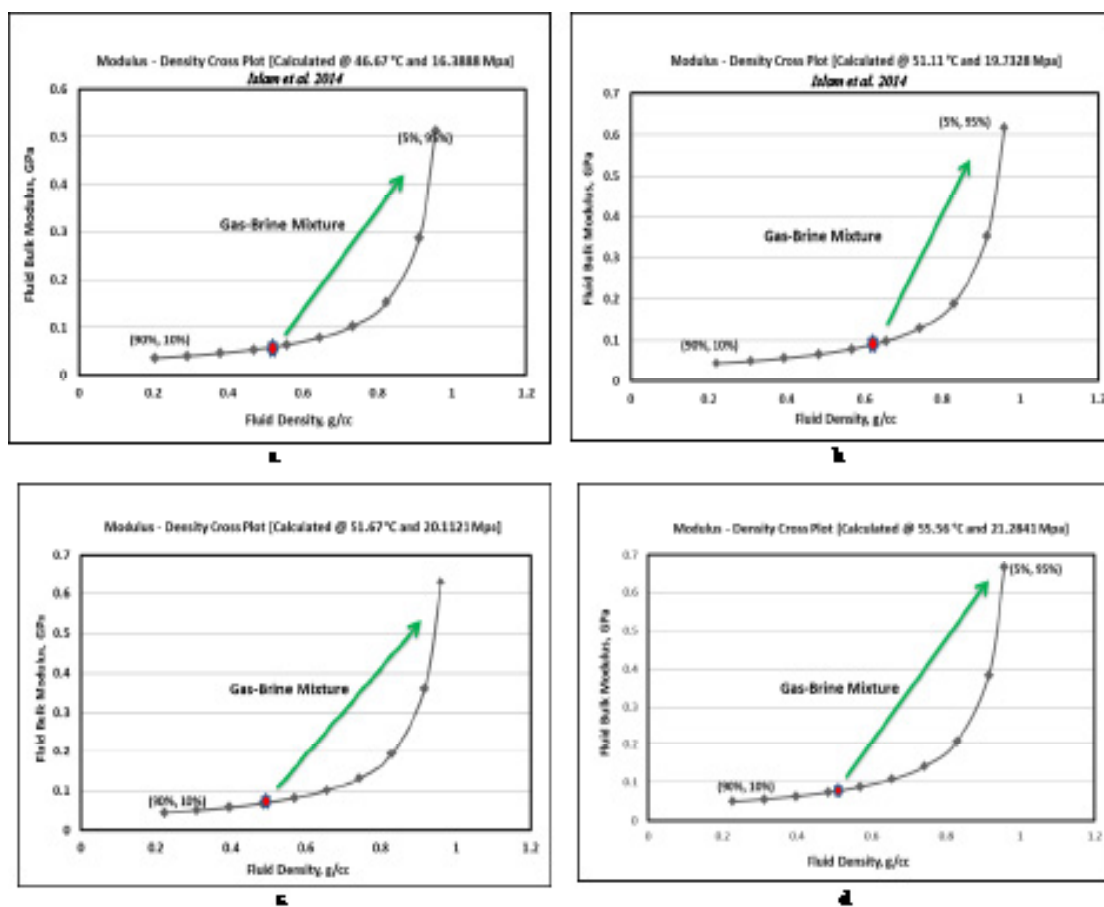


Figure 2: Cross-plot of fluid modulus and density as saturation values change (gas%, brine%) for a) New Gas Zone III, b) New Gas Zone II, c) Upper Gas Zone and d) New Gas Zone I.

Input Parameter	New Gas Zone III	New Gas Zone II	Upper Gas Zone	New Gas Zone I
Depth (m)	1656-1680	1992-2017	2030-2086	2148-2154
Pressure (MPa)	16.3888	19.7328	20.112	21.2841
Temperature (°C)	46.67	51.11	51.67	55.56
Solid Material Bulk Modulus (Gpa)	30	30	30	30
Solid Material Density (g/cc)	2.829	2.4577	2.772	2.75
Water Bulk Modulus (K_w)	2.483 GPa	2.523 GPa	2.529	2.549
Water Density (ρ_w)	1.002 g/cc	1.002 g/cc	1.002	1.002
Hydrocarbon Bulk Modulus (K_{hyd})	0.032 Gpa	0.040Gpa	0.042	0.044
Hydrocarbon Density (ρ_{hyd})	0.115 g/cc	0.1346 g/cc	0.137	0.141
Logged P-wave velocity (V_{pi})	2650 m/s	2540 m/s	2850	2180
Logged S-wave velocity (V_{si})	1606 m/s	1540 m/s	1730	1320
Logged Bulk Density (ρ_{si})	2.2 g/cc	2.2 g/cc	2.2	2.2
Fluid Bulk Modulus at logged condition (K_f)	0.584 Gpa	1.0878 Gpa	0.680	0.766

Table 5: Input values of Gassmann-Biot model (for varying saturation with constant pressure).

In this paper, we have assumed full water (wet) and gas saturation is 95% water and 90% gas, respectively. We also considered the irreducible gas saturation or depleted reservoir condition at 20% gas or 80% water (Figure 6 and Figure 7).

Based on the theory on pore fluid distribution in pore space, it is resolved that pore fluid should rise compressional velocity and decline slightly shear velocity of the rocks [2,3]. Moreover, experimental results also demonstrate that compressional and shear velocity are related to saturation [18,19]. According to Gregory [21], the saturation has larger effect on rock velocities in low porosity rocks than that of rock with high porosity. VP in fully water-saturated rocks is apparently larger than those in partially water-saturated rocks. V_s do not always fall with the rise of saturation. Instead V_s is related with pressure, porosity and the chemical interactions between pore fluid and rock skeleton. Our modeling result also displays (Figure 3) the compressional velocity (V_p , blue curve) increases with the increasing water saturation.

The compressional wave velocity (V_p , blue curve) trends from 6098 m/s, 4123 m/s, 6012 m/s and 4636 m/s at full water saturation to 3860 m/s, 2730 m/s, 4079 m/s and 2838 m/s at full gas saturation for New Gas Zone III, New Gas Zone II, Upper Gas Zone and New Gas Zone I, respectively.

During the production for upper Gas Zone and New Gas Zone I the water saturation varies from water saturation 40% to 80% and 43% to 80% respectively at reservoir conditions. Within this saturation range a significant variations has been found in the compressional velocity (20.67% and 24.68% for Upper Gas Zone and New Gas Zone I, respectively (Table 6).

The Figures 4a-d and Figures 4i-l show that the bulk density and PR increase linearly with the increase of water saturation. The bulk density (blue line in Figures 4a-d) increases from 2.1999 and 2.1948 g/cm³ to 2.2866 and 2.2737 g/cm³, respectively for Upper Gas Zone and New Gas Zone I with the water saturation increases from reservoir condition to irreducible gas saturation (20% gas). Similarly, for Upper Gas Zone and New Gas Zone, IPR (blue line in Figures 4i-j) values are trending from 0.457 and 0.458 at full water saturation to 0.386 and 0.356, at full gas saturation, respectively. The acoustic impedance (blue line in Figures 4e-h) values are increased with the increasing water saturation. The properties of the pore fluids have amplitude variation with offset at the interface between the overlying shale and the reservoir [11]. The acoustic impedance values are trending from 13941 and 10688 m/s*g/cm³ at full water saturation to 8710 and 6033 m/s*g/cm³ at full gas saturation for Upper Gas Zone and New Gas Zone I, respectively. The point labeled (green mark) reservoir conditions in Figure 5 is related to point labeled

(red mark) in Figures 3a-d. If the water saturation increases, the fluid bulk modulus and density increase, according to the green marked direction in Figs.3a-d, it has an increasing effect on PR and the acoustic impedance, and it can clearly identify from Figures 5a-h is a cross-plot of the compressional velocity of a compressional wave passing through the fluid and rock matrix versus the bulk density. These Figures show the changes in velocity and density values as the reservoir becomes increasingly water saturated. It is easily recognizable from the Figures 5e-h that compressional wave velocity and bulk density increases as water saturation increases. However, the Figures 5i-j is a cross-plot of shear wave velocity versus compressional wave velocity is consistent with the finding of Batzle and Wang model (Figures 3a-d).

Fluid models for varying saturation and pressure

Batzle and Wang model: In this section, we considered gas saturation would change from 90% to 10% at reservoir pressure of 2000 psi, 1500 psi and 1000 psi pressure for New Gas Zone III and at reservoir pressure of 2500 psi, 2000 psi, 1500 psi and 1000 psi for New Gas Zone II, Upper Gas Zone and New Gas Zone I. For different saturation and pressure conditions the moduli and densities were calculated from this model are listed (Table 7).The cross plot between fluid modulus and density versus pressure shows that the fluids have a wide range of fluid moduli and densities of different saturation conditions (Figure 6). The different fluid moduli and densities for the initial reservoir pressure conditions are shown by the yellow diamonds. The red diamond indicates the initial saturation point in the yellow line. The light brown diamond series is for 17.236893 MPa (2500 psi), dark brown series is for 3.789514 MPa (2000 psi), blue diamond series is for 10.342136 MPa (1500 psi) and the last black diamond series is for 6.894757 MPa (1000 psi) pressure. For New Gas Zone III, we assumed that during production fluid saturations (Gas: Brine) would (0.54: 0.46), (0.50: 0.50), (0.40: 0.60) and (0.30: 0.70) at different pressure line, respectively. Similarly, during production we assumed fluid saturations (Gas: Brine) would (0.36: 0.64), (0.32: 0.68), (0.28: 0.72), (0.24: 0.76) and (0.20: 0.80) for New Gas Zone II; (0.60: 0.40), (0.50: 0.50), (0.40: 0.60), (0.30: 0.70) and (0.20: 0.80) for Upper Gas Zone and (0.57: 0.43), (0.50: 0.50), (0.40: 0.60), (0.30: 0.70) and (0.20: 0.80) for New Gas Zone I at 19.737279 MPa (2862 psi), 17.236893 MPa (2500 psi), 13.789514 MPa (2000 psi), 10.342136 MPa (1500 psi) and 6.894757 MPa (1000 psi) pressure, respectively. The dry frame modulus is held constant. Figures 6a-d is showing the predicted fluid modulus path versus pressure. The black connecting line with arrow head shows the downward curve for the decreasing value of fluid modulus with respect to pressure fall during production. The fluid modulus increases with water saturation at a constant pressure, but decreases with pressure fall and overall it

Zones	Water Saturation, ρ_w	Dry Frame Rigidity, G	Bulk Density, g/cm ³	Fluid Bulk Modulus, K_f	Saturated Bulk Modulus, K_b	P-Wave Velocity, V_p	S-Wave Velocity, V_s	Poisson's Ratio, σ	Acoustic impedance, AI
New Gas Zone III (Islam et al. 2014)	0.1	5.67431	2.11280	0.03536	23.9203	3860.38	1638.80	0.39008	8156.221
	0.2	5.67431	2.13701	0.03971	26.0534	3966.33	1629.49	0.39847	8476.134
	0.3	5.67431	2.16123	0.04528	28.6042	4090.94	1620.34	0.40696	8841.479
	0.4	5.67431	2.18544	0.05267	31.7087	4239.21	1611.33	0.41556	9264.569
	0.46	5.67431	2.19997	0.05838	33.9173	4342.36	1606.00	0.42076	9553.107
	0.5	5.67431	2.20966	0.06294	35.5690	4418.25	1602.48	0.42426	9762.856
	0.6	5.67431	2.23387	0.07818	40.4996	4638.59	1593.77	0.43307	10362.06
	0.7	5.67431	2.25809	0.10316	47.0172	4916.51	1585.20	0.44199	11101.95
	0.8	5.67431	2.28230	0.15159	56.0348	5278.9	1576.77	0.45102	12048.07
	0.9	5.67431	2.30652	0.28574	69.3323	5774.02	1568.47	0.46016	13317.93
0.95	5.67431	2.31863	0.51251	78.6664	6098.44	1564.37	0.46478	14140.03	
New Gas Zone II (Islam et al. 2014)	0.1	5.21752	2.13342	0.044669	8.940381	2729.727	1563.842	0.255723	5823.6798
	0.2	5.21752	2.14600	0.050141	9.758707	2790.889	1559.252	0.273109	5989.2691
	0.3	5.21752	2.15858	0.057142	10.74193	2863.418	1554.703	0.290983	6180.9366
	0.4	5.21752	2.17116	0.066415	11.94548	2950.592	1550.192	0.309366	6406.2241
	0.5	5.21752	2.18374	0.079281	13.45275	3057.135	1545.721	0.32828	6676.0001
	0.6	5.21752	2.19632	0.098329	15.39533	3190.143	1541.289	0.347748	7006.5846
	0.64	5.21752	2.20135	0.108784	16.33908	3253.07	1539.526	0.355696	7161.1596
	0.7	5.21752	2.20890	0.129425	17.99361	3360.853	1536.894	0.367795	7423.7942
	0.8	5.21752	2.221	0.189	21.647	3588.306	1532.536	0.388448	7971.3515
	0.9	5.21752	2.234	0.352	27.162	3907.938	1528.216	0.4097	8730.564
0.95	5.21752	2.240	0.618	31.127	4122.973	1526.069	0.4206	9236.897	
Upper Gas Zone	0.1	6.584	2.135	0.046	26.750	4079.329	1756.118	0.3863	8709.550
	0.2	6.584	2.157	0.051	28.941	4182.081	1747.284	0.3943	9019.453
	0.3	6.584	2.178	0.058	31.523	4301.311	1738.581	0.4024	9369.696
	0.4	6.584	2.199	0.068	34.610	4441.031	1730.007	0.4106	9770.179
	0.45	6.584	2.211	0.074	36.393	4520.222	1725.768	0.4147	9993.318
	0.5	6.584	2.222	0.081	38.369	4606.763	1721.559	0.4188	10234.5
	0.6	6.584	2.243	0.101	43.043	4806.35	1713.233	0.4272	10781.941
	0.7	6.584	2.265	0.132	49.013	5051.368	1705.027	0.4357	11440.92
	0.8	6.584	2.287	0.194	56.907	5359.754	1696.938	0.4443	12255.399
	0.9	6.584	2.308	0.360	67.832	5761.109	1688.963	0.4529	13297.821
0.95	6.584	2.319	0.630	75.033	6011.745	1685.017	0.4574	13941.403	
New Gas Zone I	0.1	3.834	2.124	0.049	12.00	2838.39	1343.296	0.3557	6029.75
	0.2	3.834	2.146	0.0559	13.13	2915.788	1336.600	0.3670	6256.387
	0.3	3.834	2.167	0.063	14.492	3007.705	1330.003	0.3785	6517.791
	0.4	3.834	2.188	0.073	16.169	3118.338	1323.503	0.3901	6824.076
	0.43	3.834	2.195	0.077	16.750	3156.022	1321.572	0.3937	6926.744
	0.5	3.834	2.209	0.087	18.28	3253.783	1317.097	0.4020	7189.907
	0.6	3.834	2.231	0.108	21.034	3423.285	1310.784	0.4141	7637.504
	0.7	3.834	2.252	0.142	24.759	3641.682	1304.56	0.4264	8202.464
	0.8	3.834	2.273	0.207	30.089	3934.61	1298.424	0.4389	8946.205
	0.9	3.834	2.295	0.383	38.341	4351.188	1292.374	0.4516	9986.234
0.95	3.834	2.306	0.665	44.434	4635.504	1289.381	0.4581	10688.21	

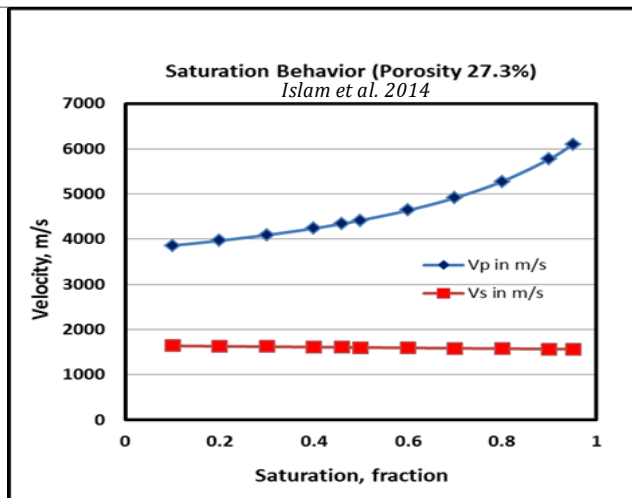
Table 6: Calculated values of Gassmann-Biot model (for varying saturation with constant pressure).

decreases through the assumed production path. So, the effect of pressure fall is dominating here for fluid modulus changes.

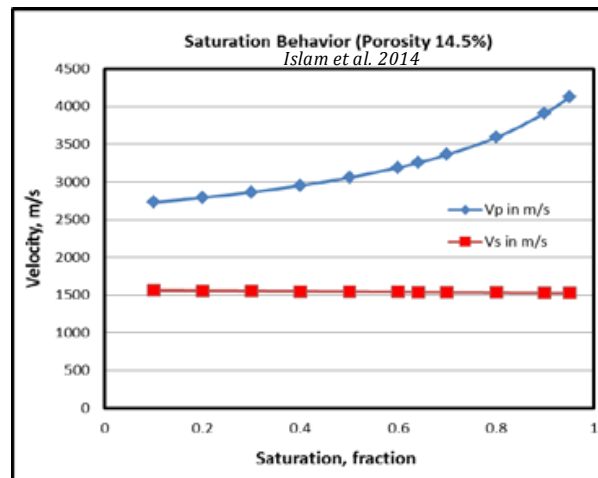
However, a reverse condition has been seen from the Figures 6e-h, which indicates that the fluid density of the reservoir is not affected as strongly as the modulus by pressure changes and variations of saturation. The density is increasing with the increase of water saturation and decreases with pressure fall for both gas zones.

Gassmann-Biot Model: In this section, the initial conditions of the Figs. are same as the Figure 6. All the outputs from Gassmann-Biot model are listed in Table 8. As we know that the Biot- Gassmann theory precisely forecasts velocity ratios with respect to differential pressure

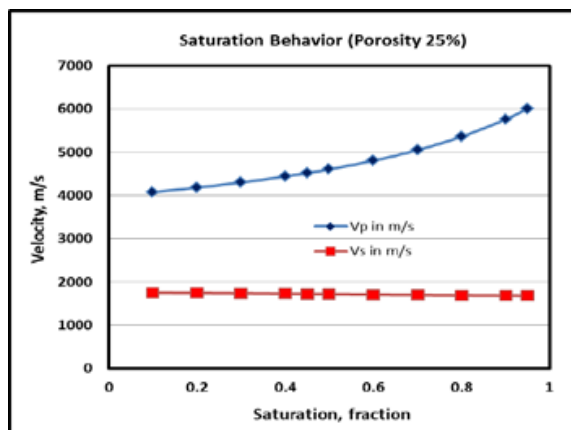
for given porosity. However, because the velocity ratio is weakly associated to porosity, it is not suitable to investigate the velocity ratio with respect to porosity (ϕ). The velocity ratio has been used for many purposes, such as a lithology indicator, determining degree of consolidation, identifying pore fluid, and predicting velocities [18-20]. The velocity ratio usually depends on porosity, degree of consolidation, clay content, differential pressure, pore geometry, and other factors. The velocity ratio for dry rock or gas-saturated rock is almost a constant regardless of porosity and differential pressure, whereas the velocity ratio of wet rock depends significantly on porosity and differential pressure. P-wave to S-wave velocity ratio (V_p/V_s) for the all gas zones Fenchuganj Gas Field show value of more than 2.0 which show the



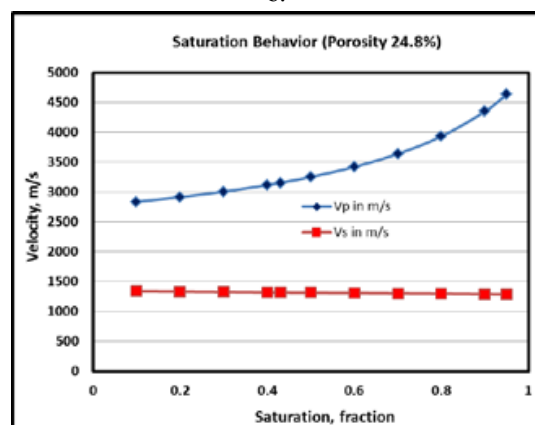
a.



b.

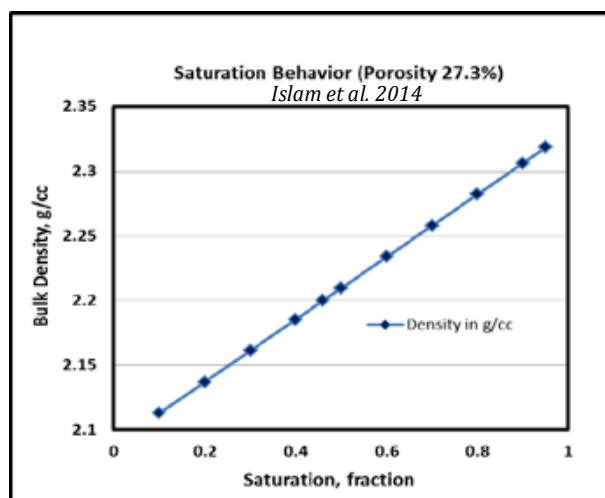


c.

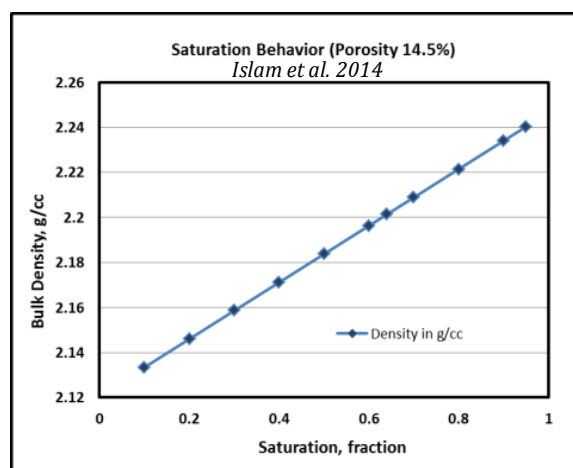


d.

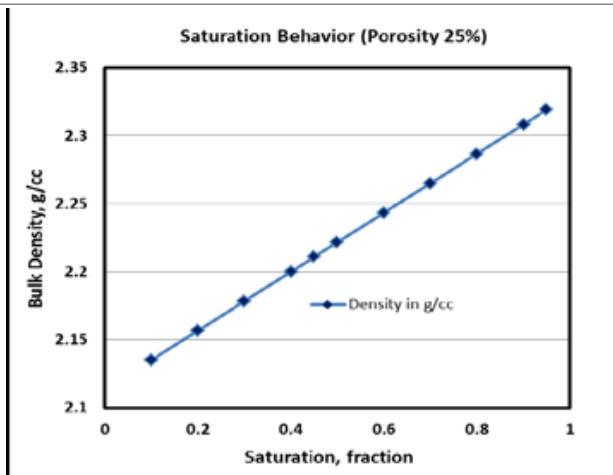
Figure 3: Velocity versus saturation shows how water saturation affects a two phase mixture of gas and brine in a sandstone matrix from water to gas saturated conditions for a) New Gas Zone III, b) New Gas Zone II, c) Upper Gas Zone and d) New Gas Zone I.



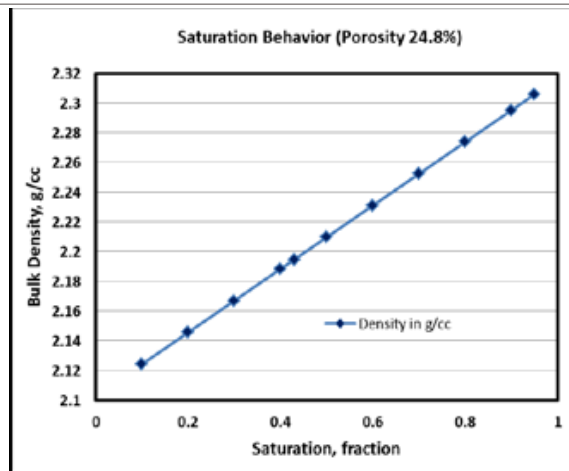
a.



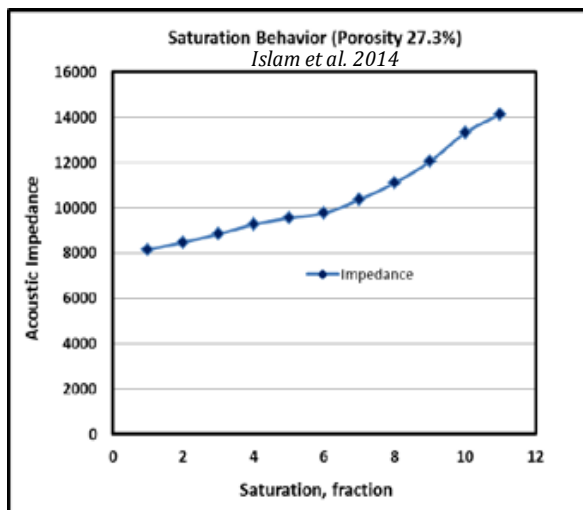
b.



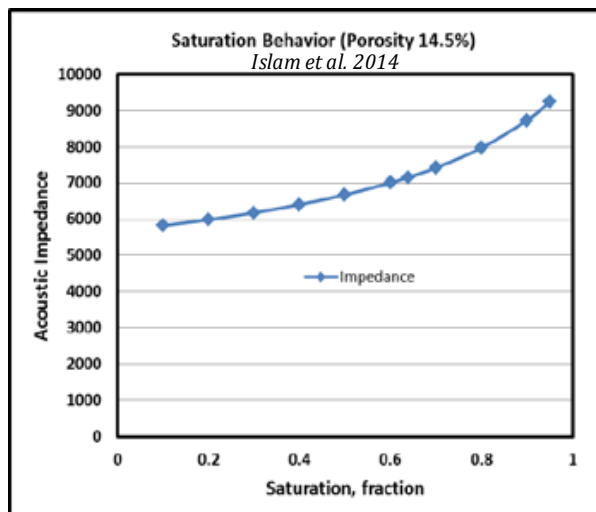
c.



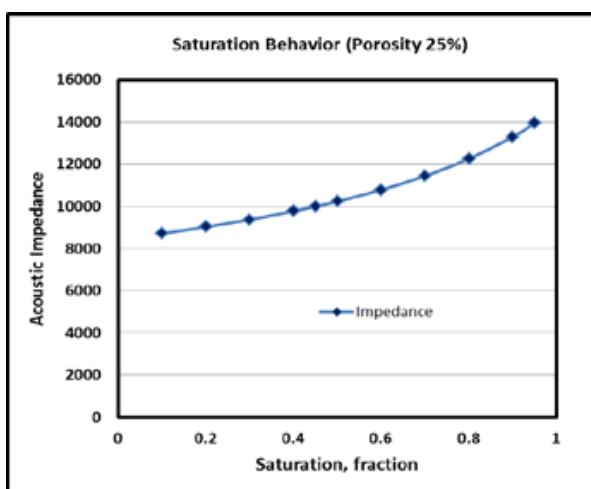
d.



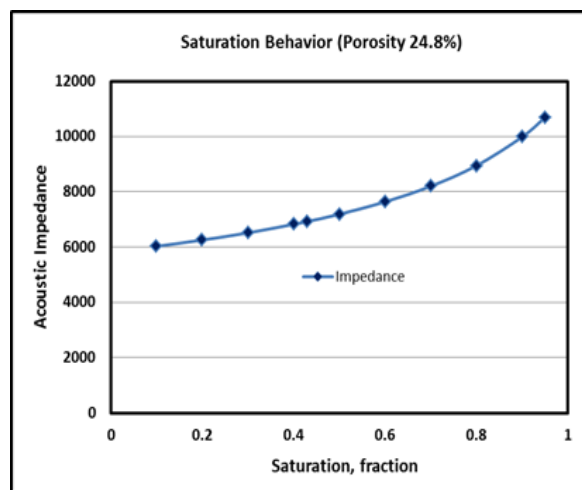
e.



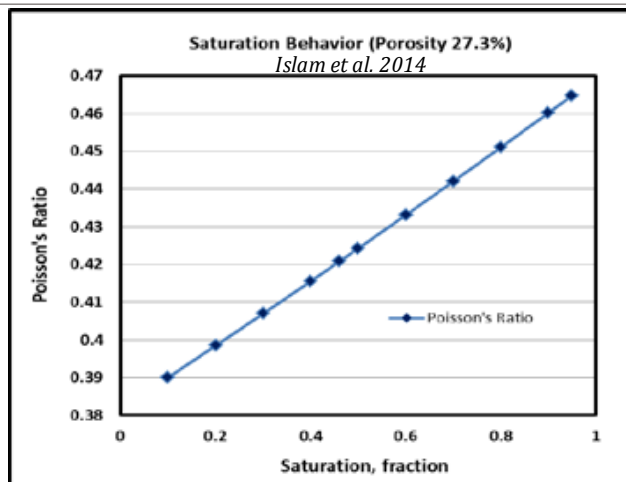
f.



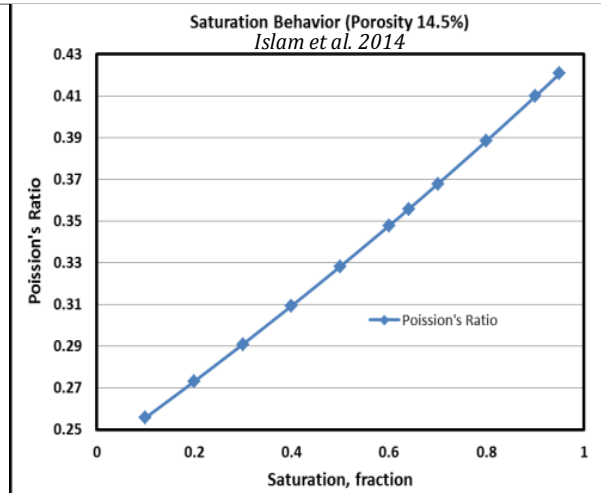
g.



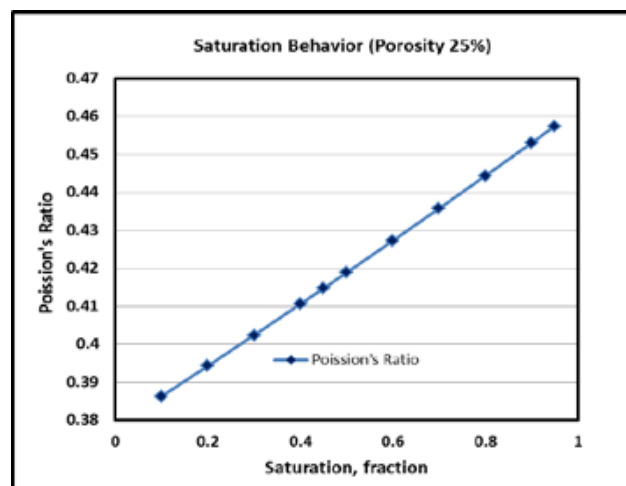
h.



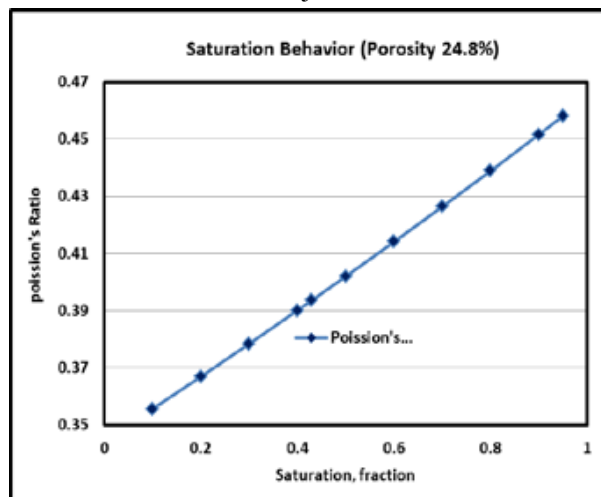
i.



j.

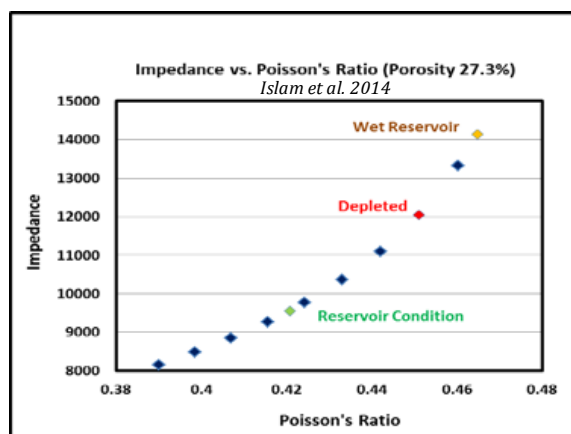


k.

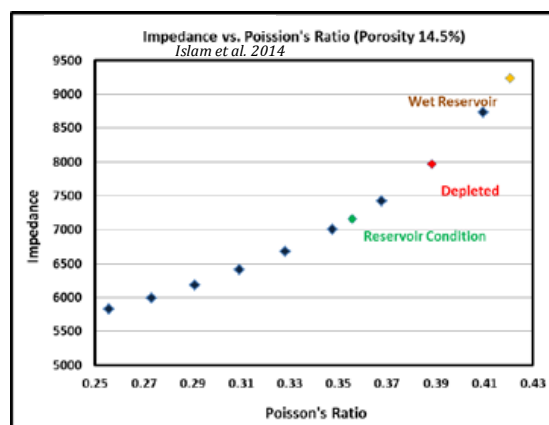


l.

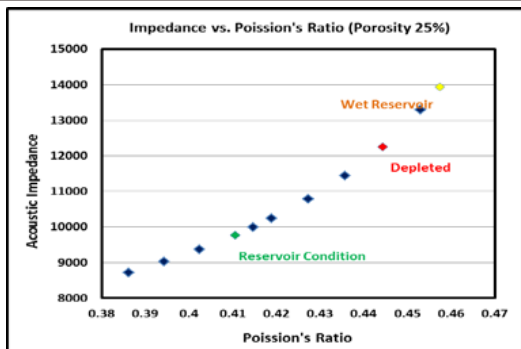
Figure4: (a-d) Bulk density versus saturation; (e-h) Acoustic Impedance versus saturation; and (i-l) Poisson's ratio versus saturation shows how water saturation affects a two phase mixture of gas and brine in a sandstone matrix from water to gas saturated conditions.



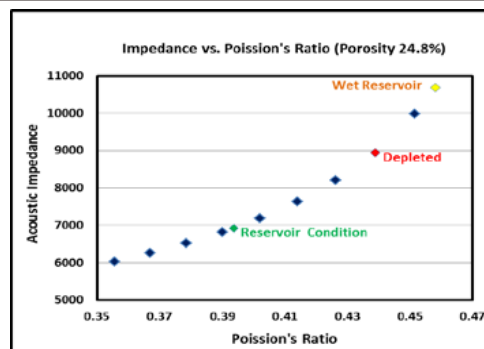
a.



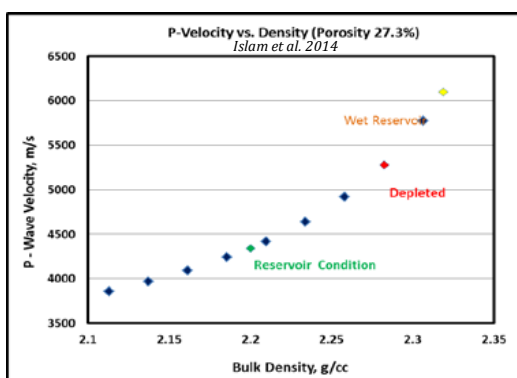
b.



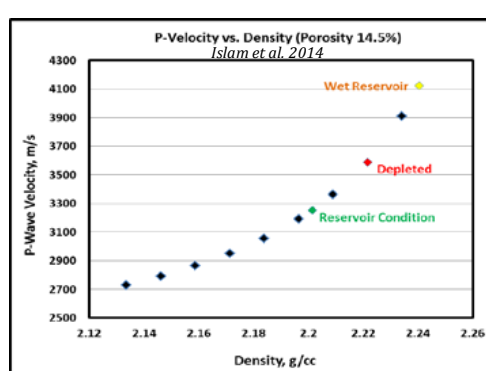
c.



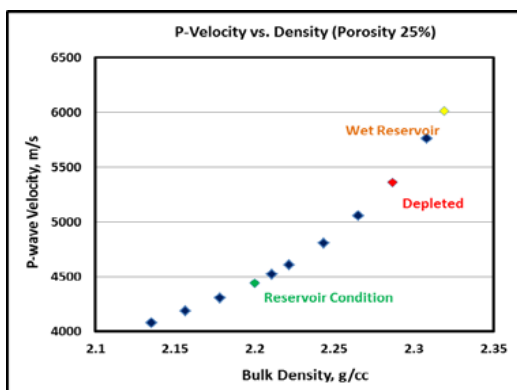
d.



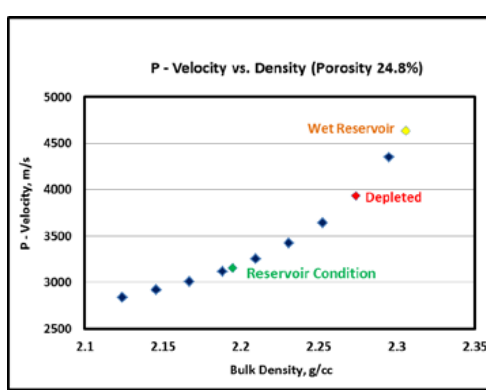
e.



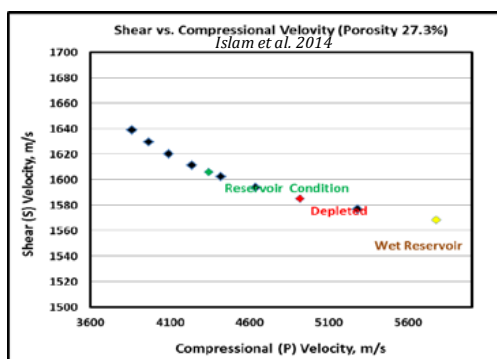
f.



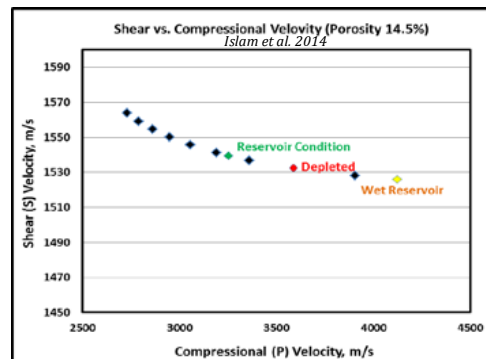
g.



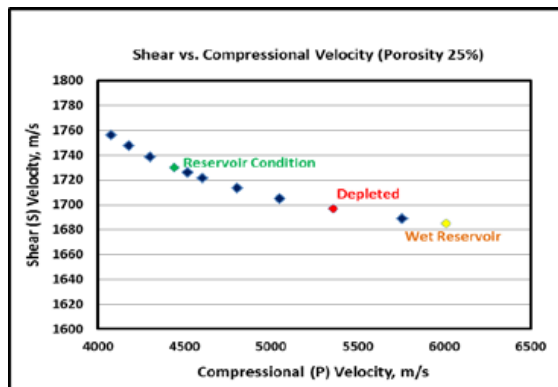
h.



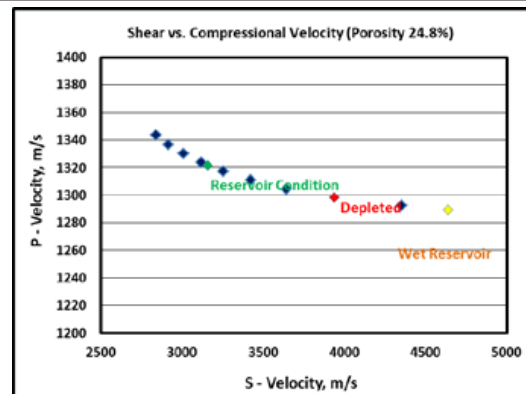
i.



j.



k.



l.

Figure 5: (a-d) Acoustic impedance Vs. Poisson's ratio cross-plot; (e-h) Compressional wave velocity Vs. Bulk density cross-plot; (i-j) Shear wave velocity Vs. Compressional wave velocity cross-plot for a two phase mixture of gas and brine in a sandstone matrix from water to gas saturated conditions

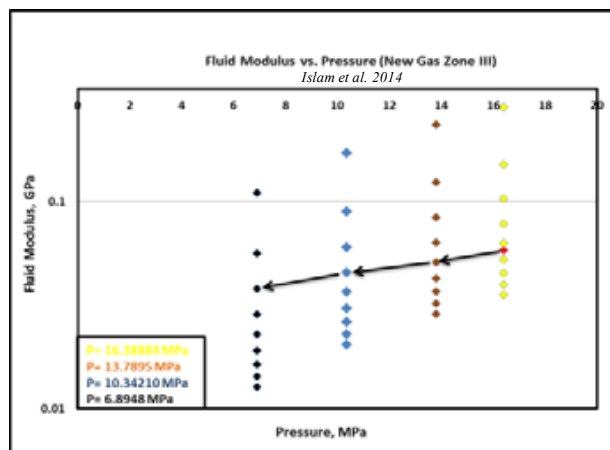
Calculation for New Gas Zone III (Islam et al. 2014)							
Pressure: 16.38884 Mpa (2377psi)				Pressure: 13.7895Mpa (2000psi)			
Density of Gas: 0.115 g/cc				Density of Gas: 0.0963 g/cc			
Modulus of Gas: 0.031754 Gpa				Modulus of Gas: 0.025795 Gpa			
Density of Brine: 1.0019 g/cc				Density of Brine: 1.0008 g/cc			
Modulus of Brine: 2.483332 Gpa				Modulus of Brine: 2.466893 Gpa			
Gas%	Brine%	Density, g/cc	Modulus, Gpa	Gas%	Brine%	Density, g/cc	Modulus, Gpa
90	10	0.2038	0.035	90	10	0.1868	0.029
80	20	0.2924	0.039	80	20	0.2772	0.032
70	30	0.3811	0.045	70	30	0.3677	0.037
60	40	0.4698	0.053	60	40	0.4581	0.043
54	46	0.523	0.059	50	50	0.5486	0.051
50	50	0.5585	0.063	40	60	0.639	0.063
40	60	0.6472	0.078	30	70	0.7295	0.084
30	70	0.7359	0.103	20	80	0.8199	0.124
20	80	0.8246	0.152	10	90	0.9104	0.236
10	90	0.9132	0.286				
Pressure: 10.3421Mpa(1500psi)				Pressure: 6.8948Mpa(1000psi)			
Density of Gas: 0.0707g/cc				Density of Gas: 0.0454g/cc			
Modulus of Gas: 0.018361Gpa				Modulus of Gas: 0.011486Gpa			
Density of Brine: 0.9994g/cc				Density of Brine: 0.9979g/cc			
Modulus of Brine: 2.445394Gpa				Modulus of Brine: 2.424272Gpa			
Gas%	Brine%	Density, g/cc	Modulus, Gpa	Gas%	Brine%	Density, g/cc	Modulus, Gpa
90	10	0.1636	0.0204	90	10	0.1407	0.0128
80	20	0.2563	0.0229	80	20	0.2359	0.0143
70	30	0.3493	0.0261	70	30	0.3312	0.0164
60	40	0.4422	0.0304	60	40	0.4264	0.0191
50	50	0.5351	0.0364	50	50	0.5217	0.0229
40	60	0.6279	0.0454	40	60	0.6169	0.0285
30	70	0.7208	0.0601	30	70	0.7122	0.0379
20	80	0.8137	0.0891	20	80	0.8075	0.0564
10	90	0.9065	0.1719	10	90	0.9027	0.1102
Calculation for New Gas Zone II (Islam et al. 2014)							
Pressure: 19.73279Mpa(2862psi)				Pressure: 17.236893Mpa(2500psi)			
Density of Gas: 0.1346g/c				Density of Gas: 0.1182g/cc			
Modulus of Gas: 0.040273Gpa				Modulus of Gas: 0.033909Gpa			
Density of Brine: 1.0022g/cc				Density of Brine: 1.0012g/cc			
Modulus of Brine: 2.523198Gpa				Modulus of Brine: 2.506883Gpa			
Gas%	Brine%	Density, g/cc	Modulus, Gpa	Gas%	Brine%	Density, g/cc	Modulus, Gpa
90	10	0.2214	0.0447	90	10	0.2065	0.0376
80	20	0.3081	0.0501	80	20	0.2948	0.0422
70	30	0.3949	0.0571	70	30	0.3831	0.0482

60	40	0.4817	0.0664	60	40	0.4714	0.0560
50	50	0.5684	0.0793	50	50	0.5597	0.0669
40	60	0.6552	0.0983	40	60	0.6479	0.08309
36	64	0.6899	0.1088	30	70	0.7363	0.1096
30	70	0.7419	0.1294	20	80	0.8246	0.1608
20	80	0.8286	0.1893	10	90	0.9129	0.3023
10	90	0.9154	0.3521				
Pressure: 13.789514 Mpa (2000psi)				Pressure: 10.342136 Mpa (1500psi)			
Density of Gas: 0.0941 g/cc				Density of Gas:0.0692 g/cc			
Modulus of Gas: 0.025843 Gpa				Modulus of Gas: 0.018437 Gpa			
Density of Brine: 0.9998 g/cc				Density of Brine: 0.9983 g/cc			
Modulus of Brine:2.484589 Gpa				Modulus of Brine: 2.462607 Gpa			
Gas%	Brine%	Density, g/cc	Modulus, Gpa	Gas%	Brine%	Density, g/cc	Modulus, Gpa
90	10	0.1847	0.0229	90	10	0.1621	0.0205
80	20	0.2752	0.0322	80	20	0.255	0.0230
70	30	0.3658	0.0368	70	30	0.3479	0.0262
60	40	0.4564	0.0428	60	40	0.4408	0.0306
50	50	0.5469	0.0512	50	50	0.5338	0.0366
40	60	0.6375	0.0636	40	60	0.6267	0.0456
30	70	0.7281	0.0841	30	70	0.7196	0.0604
20	80	0.8186	0.1241	20	80	0.8125	0.0895
10	90	0.9092	0.2363	10	90	0.9054	0.1727
Pressure:6.894757Mpa(1000psi)				Density of Brine:0.9969g/cc			
Density of Gas:0.0445g/cc				Modulus of Brine:2.440969Gpa			
Modulus of Gas:0.011539Gpa							
Gas%	Brine%	Density, g/cc	Modulus, Gpa	Gas%	Brine%	Density, g/cc	Modulus, Gpa
90	10	0.1397	0.0128				
80	20	0.2349	0.0144				
70	30	0.3302	0.0164				
60	40	0.4255	0.0192				
50	50	0.5207	0.0229				
40	60	0.6159	0.0286				
30	70	0.7112	0.0381				
20	80	0.8064	0.0566				
10	90	0.9017	0.1107				
Calculation for Upper Gas Zone							
Pressure: 20.112006 Mpa (2917 psi)				Pressure: 17.236893 Mpa (2500 psi)			
Density of Gas: 0.1367 g/cc				Density of Gas: 0.1178 g/cc			
Modulus of Gas: 0.041259 Gpa				Modulus of Gas: 0.033904 Gpa			
Density of Brine: 1.0025 g/cc				Density of Brine: 1.0013 g/cc			
Modulus of Brine: 2.529461 Gpa				Modulus of Brine: 2.510602 Gpa			
Gas%	Brine%	Density, g/cc	Modulus, Gpa	Gas%	Brine%	Density, g/cc	Modulus, Gpa
90	10	0.2232	0.045761	90	10	0.2062	0.037615
80	20	0.3098	0.051365	80	20	0.2945	0.042238
70	30	0.3964	0.058533	70	30	0.3829	0.048156
60	40	0.4829	0.068026	60	40	0.4712	0.056003
50	50	0.5696	0.081194	50	50	0.5596	0.066905
40	60	0.6561	0.100685	40	60	0.6479	0.083077
30	70	0.7427	0.132489	30	70	0.7363	0.109561
20	80	0.8293	0.193661	20	80	0.8246	0.160833
10	90	0.9159	0.35977	10	90	0.9129	0.302299
Pressure: 13.789514 Mpa(2000 psi)				Pressure: 10.342136 Mpa (1500 psi)			
Density of Gas: 0.0938 g/cc				Density of Gas: 0.0689 g/cc			
Modulus of Gas: 0.025849 Gpa				Modulus of Gas: 0.018447 Gpa			
Density of Brine: 0.9999 g/cc				Density of Brine: 0.9985 g/cc			
Modulus of Brine: 2.488241 Gpa				Modulus of Brine: 2.466185 Gpa			
Gas%	Brine%	Density, g/cc	Modulus, Gpa	Gas%	Brine%	Density, g/cc	Modulus, Gpa
90	10	0.1844	0.0287	90	10	0.1619	0.0205
80	20	0.275	0.0322	80	20	0.2549	0.0230
70	30	0.3656	0.0368	70	30	0.3478	0.0263
60	40	0.4562	0.0428	60	40	0.4408	0.0306

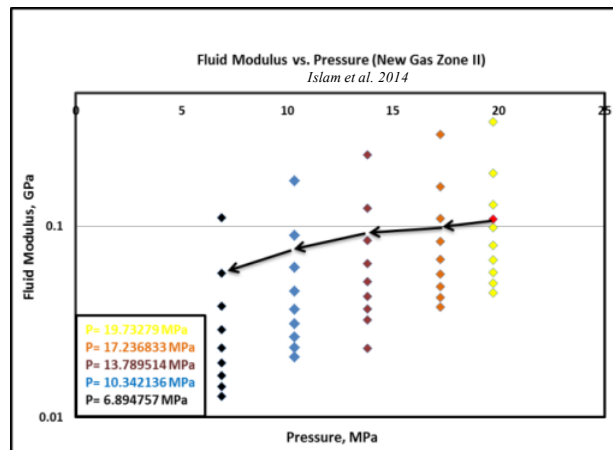
50	50	0.5469	0.0512	50	50	0.5337	0.0367
40	60	0.6375	0.0636	40	60	0.6267	0.0456
30	70	0.7281	0.084123	30	70	0.7196	0.0604
20	80	0.8187	0.1281	20	80	0.8126	0.0895
10	90	0.9093	0.2364	10	90	0.9055	0.1728
Pressure: 6.894757 Mpa (1000 psi)							
Density of Gas: 0.0444 g/cc				Density of Brine: 0.9970 g/cc			
Modulus of Gas: 0.011546 Gpa				Modulus of Brine: 2.444469 Gpa			
Gas%	Brine%	Density, g/cc	Modulus, Gpa	Gas%	Brine%	Density, g/cc	Modulus, Gpa
90	10	0.1397	0.0128	90	10	0.1397	0.0128
80	20	0.2349	0.0144	80	20	0.2349	0.0144
70	30	0.3302	0.0165	70	30	0.3302	0.0165
60	40	0.4254	0.0192	60	40	0.4254	0.0192
50	50	0.5267	0.0229	50	50	0.5267	0.0229
40	60	0.6159	0.0286	40	60	0.6159	0.0286
30	70	0.7112	0.0381	30	70	0.7112	0.0381
20	80	0.8065	0.0567	20	80	0.8065	0.0567
10	90	0.9018	0.1108	10	90	0.9018	0.1108
Calculation for New Gas Zone I							
Pressure: 21.284115 Mpa (3087 psi)				Pressure: 17.236893 Mpa (2500 psi)			
Density of Gas: 0.1412 g/cc				Density of Gas: 0.1155 g/cc			
Modulus of Gas: 0.044235 Gpa				Modulus of Gas: 0.033871 Gpa			
Density of Brine: 1.0017 g/cc				Density of Brine: 0.9999 g/cc			
Modulus of Brine: 2.548473 Gpa				Modulus of Brine: 2.521438 Gpa			
Gas%	Brine%	Density, g/cc	Modulus, Gpa	Gas%	Brine%	Density, g/cc	Modulus, Gpa
90	10	0.2272	0.0491	90	10	0.2065	0.0376
80	20	0.3133	0.0551	80	20	0.2948	0.0422
70	30	0.3993	0.0627	70	30	0.3831	0.0482
60	40	0.4854	0.0729	60	40	0.4714	0.0560
57	43	0.5112	0.0766	50	50	0.5597	0.0669
50	50	0.5714	0.0869	40	60	0.6479	0.0831
40	60	0.6474	0.1078	30	70	0.7363	0.1096
30	70	0.7435	0.1417	20	80	0.8246	0.1608
20	80	0.8295	0.2068	10	90	0.9129	0.3023
10	90	0.9156	0.3826				
Pressure: 13.789514 Mpa (2000 psi)				Pressure: 10.342136 Mpa (1500 psi)			
Density of Gas: 0.0941 g/cc				Density of Gas: 0.0692 g/cc			
Modulus of Gas: 0.025843 Gpa				Modulus of Gas: 0.018437 Gpa			
Density of Brine: 0.9998 g/cc				Density of Brine: 0.9983 g/cc			
Modulus of Brine: 2.484589 Gpa				Modulus of Brine: 2.462607 Gpa			
Gas%	Brine%	Density, g/cc	Modulus, Gpa	Gas%	Brine%	Density, g/cc	Modulus, Gpa
90	10	0.1847	0.0229	90	10	0.1621	0.0205
80	20	0.2752	0.0322	80	20	0.255	0.0230
70	30	0.3658	0.0368	70	30	0.3479	0.0263
60	40	0.4564	0.0428	60	40	0.4408	0.0306
50	50	0.5469	0.0512	50	50	0.5338	0.0366
40	60	0.6375	0.0636	40	60	0.6267	0.0456
30	70	0.7281	0.0841	30	70	0.7196	0.0604
20	80	0.8186	0.1241	20	80	0.8125	0.0895
10	90	0.9092	0.2363	10	90	0.9054	0.1727
Pressure: 6.894757 Mpa(1000 psi)				Density of Brine: 0.9969 g/cc			
Density of Gas: 0.0445 g/cc				Modulus of Brine: 2.440969 Gpa			
Modulus of Gas: 0.011539 Gpa				Density, g/cc			
Gas%	Brine%	Density, g/cc	Modulus, Gpa	Gas%	Brine%	Density, g/cc	Modulus, Gpa
90	10	0.1397	0.0129	90	10	0.1397	0.0129
80	20	0.2349	0.0144	80	20	0.2349	0.0144
70	30	0.3302	0.0165	70	30	0.3302	0.0165
60	40	0.4255	0.0192	60	40	0.4255	0.0192
50	50	0.5207	0.0229	50	50	0.5207	0.0229
40	60	0.6159	0.0286	40	60	0.6159	0.0286
30	70	0.7112	0.0380	30	70	0.7112	0.0380

20	80	0.8064	0.0566
10	90	0.9017	0.1107

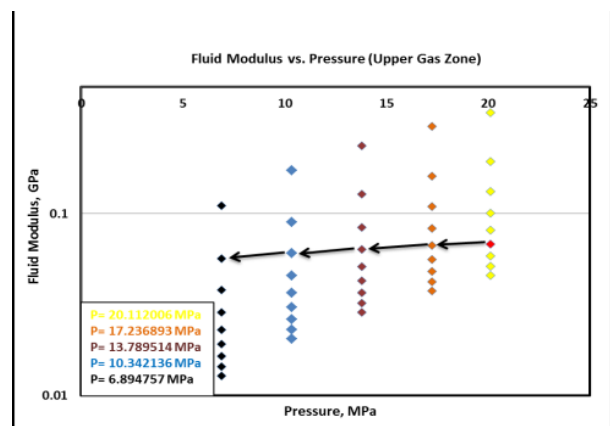
Table 7: Calculated fluid properties from Batzle and Wang Model (for varying saturation and pressure).



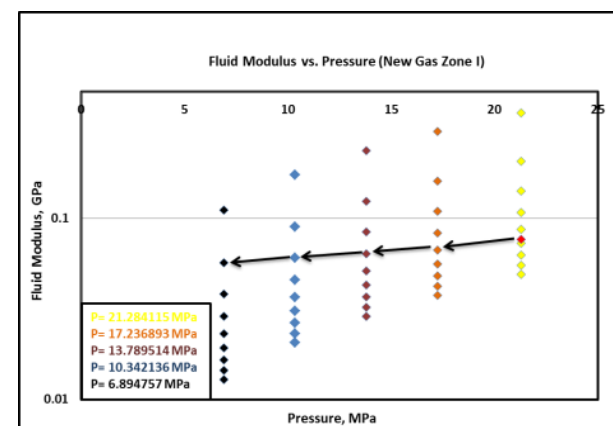
a.



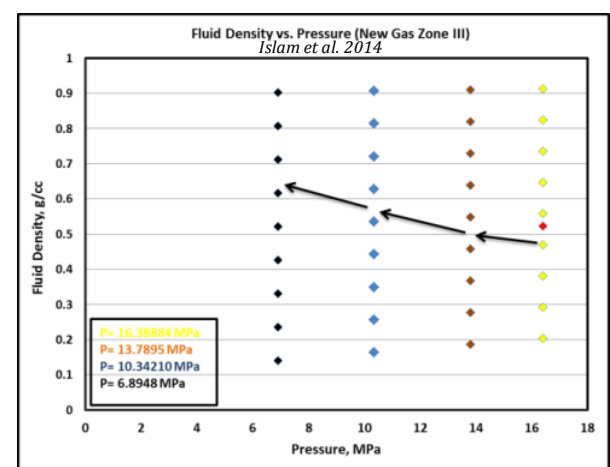
b.



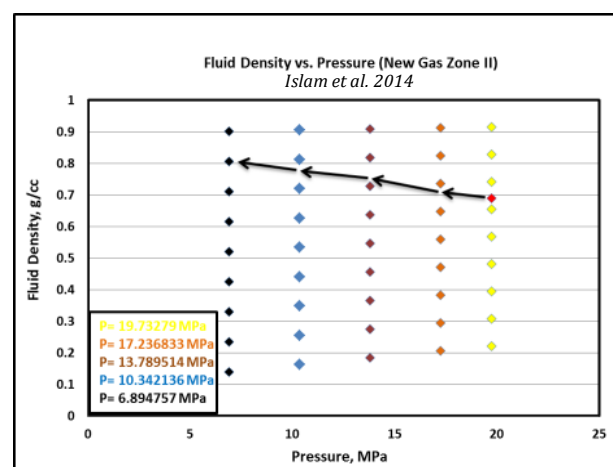
c.



d.



e.



f.

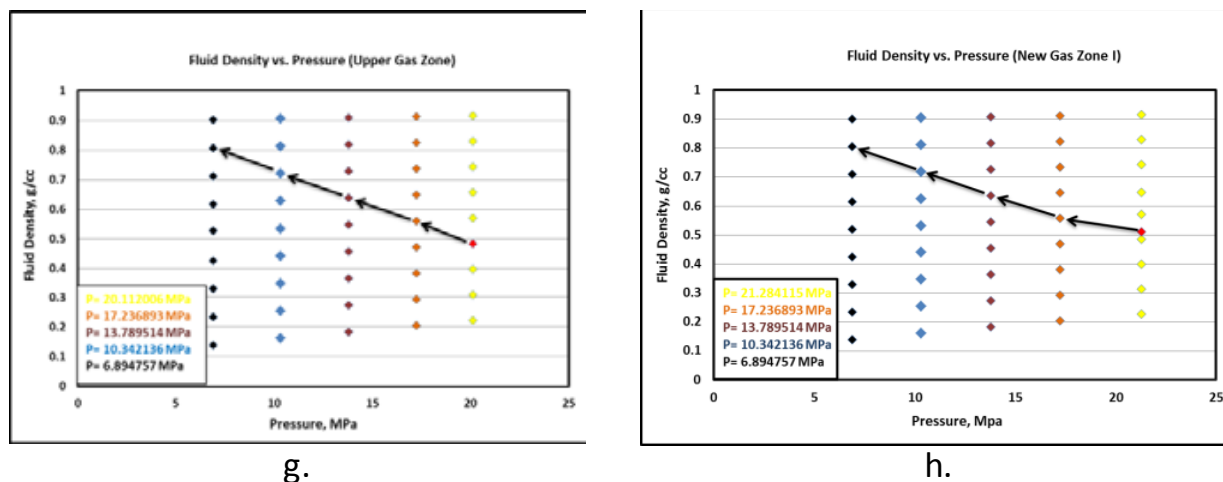


Figure 6: Fluid modulus versus pressure shows the changes in the fluid modulus as the pressure and saturation in the reservoir changes during production for a) New Gas Zone III, b) New Gas Zone II, c) Upper Gas Zone and d) (New Gas Zone I). Fluid density versus pressure shows the changes in the fluid density as the pressure and saturation in the reservoir changes during production for e) New Gas Zone III, f) New Gas Zone II, g) Upper Gas Zone and h) New Gas Zone I.

presence of gas in the unconsolidated rock [21] with higher porosity [22].

Figure 7 displays the predicted P-wave velocity, PR and acoustic impedances under differential pressure due to gas production rises. The black connecting line with arrow head displays the downward curve for the decreasing value of all parameters respects to pressure fall during production. These parameters rise with water saturation at a constant pressure, but falls with pressure drop. So, it can forecast that the New Gas Zone II has greater effect on parameters change than the other three gas zones.

AVO analysis

At this final stage, we determined and analyzed the AVO response for Upper Gas Zone and New Gas Zone I and compared with New Gas Zone III and II (AVO response for New Gas Zone III and New Gas Zone II has already published as Islam et al. 2014 [16] of Fenchuganj Gas Field. In geophysics and reflection seismology, amplitude versus offset (AVO) is the general term for referring to the dependency of the seismic attribute, amplitude, with the distance between the source and receiver (the offset). According to Schlumberger Oilfield Glossary, AVO analysis is a technique that geophysicists can execute on seismic data to determine a rock's fluid content, porosity, density or seismic velocity, shear wave information, fluid indicators. If matches with the standard figures AVO gives the validity of the reservoir properties which are used to interpret it.

Zoeppritz [1] equations provide a complete solution for amplitudes of transmitted and reflected P- and S- waves for both incident P- and S-waves. The equations are very complex and subject to troublesome sign, convention, or typographic errors. Hilterman [18], Aki and Richards [22], and Shuey [23], developed simplifications and approximations for Zoeppritz equations.

So, at first, we took assumptions given by Shuey [23] for simplification of Zoeppritz [1] equation and interpreted AVO that empirical equation for 0-30° incident angle. The phenomenon is based on the relationship between the reflection coefficient and the angle of incidence. Zoeppritz Equation:

$$R(\theta) = A + B \sin^2 \theta$$

$$A = \frac{1}{2} \left(\frac{\Delta V_p}{V_p} + \frac{\Delta \rho}{\rho} \right)$$

$$B = A_o A + \left(\frac{\Delta \sigma}{(1 - \sigma)^2} \right)$$

Where, $R(\theta)$ = reflection coefficient (function of θ), θ = angle of incidence, A = zero-offset reflection coefficient (AVO intercept) and B = slope of the amplitude (AVO Gradient).

The input values (V_p , ρ_b and σ) for AVO interpretation are taken from the output values (Table 9) of Gassmann-Biot model for varying saturation and pressure. The comparison of seismic reflection change due to a change of pressure and saturation of a definite layer from the reservoir condition are represented by every reflection curve of Figures 8c-d for Upper Gas Zone and New Gas Zone I and these two figures are similar to Figures 8a-b for New Gas Zone III and II. It is obvious that the AVO response decreases as water saturation increases. Every curve of Figures 8a-d indicates class 3 AVO.

Secondly, we have interpreted AVO without any assumptions. We used full Zoeppritz [1] equation with the help of an AVO calculator by Timothy et al. which starts with negative values and decreases with the offset indicating of low impedance gas sand class 3 AVO [11]. This characteristic of AVO indicates bright zone that is potential for hydrocarbon zone [11].

The input values used to determine AVO, were taken from the results of Gassmann-Biot model which is also dependent on outputs of Batzle and Wang model. Both approaches applied in this section, the AVO reflection indicates class 3 type and it is a good sign to be sure that Fenchuganj is a gas reservoir and ironically we know it. So, it can be inferred surely that the fluid properties we determined in previous sections by Batzle and Wang model and Gassmann-both models are fairly correct.

Conclusion

The fluid properties for both of the constant/varying saturation with constant/varying pressure condition are analyzed by the Batzle and Wang model that predicted near precise forecasting. Increase

Calculation for New Gas Zone III (Islam et al. 2014)						
Input Parameters (Fixed)				Symbol	Value	Unit
Depth				D	1656-1680	m
Temperature				T	46.67	°C
Solid Material Bulk Modulus				K_s	30	Gpa
Solid Material Density				ρ_s	2.8297	g/cc
Logged P-wave velocity				V_{pl}	2650	m/s
Logged S-wave velocity				V_{sl}	1606	m/s
Logged Bulk Density				ρ_{pl}	2.2	g/cc
Fluid Bulk Modulus at logged condition				K_f	0.5839	Gpa
Parameter(Variable)				Symbol	Value	Unit
Pressure				P	16.3884	Mpa
Water Bulk Modulus				K_w	2.483332	GPa
Water Density				ρ_w	1.0019	g/cc
Hydrocarbon Bulk Modulus				K_{hyd}	0.031754	Gpa
Hydrocarbon Density				ρ_{hyd}	0.115	g/cc
S_w	S_g	ρ_b in g/cc	V_p in m/s	V_s in m/s	σ	AI
0.1	0.9	2.113	3860.397	1638.807	0.390	8156.245
0.2	0.8	2.137	3966.357	1629.497	0.398	8476.153
0.3	0.7	2.161	4090.965	1620.343	0.407	8841.49
0.4	0.6	2.185	4239.234	1611.342	0.4157	9264.577
0.46	0.54	2.199	4342.395	1606.013	0.421	9553.111
0.5	0.5	2.209	4418.285	1602.490	0.424	9762.857
0.6	0.4	2.234	4638.628	1593.782	0.433	10362.051
0.7	0.3	2.258	4916.553	1585.214	0.442	11101.938
0.8	0.2	2.283	5278.937	1576.783	0.451	12048.043
0.9	0.1	2.307	5774.068	1568.489	0.460	13317.877
Parameter(Variable)				Symbol	Value	Unit
Pressure				P	13.7895	Mpa
Water Bulk Modulus				K_w	2.466893	GPa
Water Density				ρ_w	1.0008	g/cc
Hydrocarbon Bulk Modulus				K_{hyd}	0.025795	Gpa
Hydrocarbon Density				ρ_{hyd}	0.0963	g/cc
S_w	S_g	ρ_b in g/cc	V_p in m/s	V_s in m/s	σ	AI
0.1	0.9	2.108	3638.347	1640.603	0.372	7670.271
0.2	0.8	2.133	3739.577	1631.079	0.383	7976.023
0.3	0.7	2.157	3860.010	1621.718	0.393	8328.205
0.4	0.6	2.182	4005.194	1612.517	0.403	8740.347
0.5	0.5	2.207	4183.198	1603.471	0.414	9232.092
0.6	0.4	2.232	4406.289	1594.575	0.4246	9833.247
0.7	0.3	2.256	4694.208	1585.825	0.436	10591.69
0.8	0.2	2.281	5081.197	1577.219	0.447	11590.34
0.9	0.1	2.306	5633.261	1568.750	0.458	12988.708
Parameter(Variable)				Symbol	Value	Unit
Pressure				P	10.342	Mpa
Water Bulk Modulus				K_w	2.445	GPa
Water Density				ρ_w	0.999	g/cc
Hydrocarbon Bulk Modulus				K_{hyd}	0.0184	Gpa
Hydrocarbon Density				ρ_{hyd}	0.071	g/cc
S_w	S_g	ρ_b in g/cc	V_p in m/s	V_s in m/s	σ	AI
0.1	0.9	2.102	3308.279	1643.071	0.336	6953.495
0.2	0.8	2.1272	3398.769	1633.250	0.349	7229.865
0.3	0.7	2.1522	3508.429	1623.603	0.364	7552.081
0.4	0.6	2.178	3643.362	1614.125	0.378	7934.90
0.5	0.5	2.203	3812.755	1604.811	0.392	8400.493
0.6	0.4	2.229	4031.192	1595.657	0.407	8983.972
0.7	0.3	2.254	4323.494	1586.657	0.422	9745.014
0.8	0.2	2.280	4736.177	1577.801	0.438	10795.269
0.9	0.1	2.305	5369.751	1569.105	0.453	12375.529
Parameter(Variable)				Symbol	Value	Unit
Pressure				P	6.8948	Mpa

Water Bulk Modulus				Kw	2.424272	GPa
Water Density				ρ_w	0.9979	g/cc
Hydrocarbon Bulk Modulus				Khyd	0.011486	Gpa
Hydrocarbon Density				ρ_{hyd}	0.0454	g/cc
Sw	Sg	ρ_b in g/cc	Vp in m/s	Vs in m/s	σ	AI
0.1	0.9	2.0956	2918.857	1645.522	0.267	6116.725
0.2	0.8	2.122	2990.867	1635.407	0.287	6345.401
0.3	0.7	2.148	3080.426	1625.476	0.307	6615.509
0.4	0.6	2.174	3193.738	1615.724	0.328	6941.906
0.5	0.5	2.1994	3340.516	1606.145	0.350	7347.808
0.6	0.4	2.226	3536.966	1596.735	0.372	7871.892
0.7	0.3	2.252	3812.577	1587.488	0.395	8584.432
0.8	0.2	2.278	4228.153	1578.399	0.419	9630.092
0.9	0.1	2.304	4936.554	1569.466	0.444	11371.922
Calculation for New Gas Zone II (Islam et al. 2014)						
Input Parameters(Fixed)				Symbol	Value	Unit
Depth				D	1992-2017	m
Temperature				T	51.11	°C
Solid Material Bulk Modulus				Ks	30	Gpa
Solid Material Density				ρ_s	2.458	g/cc
Logged P-wave velocity				Vpi	2540	m/s
Logged S-wave velocity				Vsi	1540	m/s
Logged Bulk Density				ρ_{bi}	2.2	g/cc
Fluid Bulk Modulus at logged condition				Kfi	1.088	Gpa
Parameter(Variable)				Symbol	Value	Unit
Pressure				P	19.733	Mpa
Water Bulk Modulus				Kw	2.523	GPa
Water Density				ρ_w	1.0022	g/cc
Hydrocarbon Bulk Modulus				Khyd	0.040	Gpa
Hydrocarbon Density				ρ_{hyd}	0.135	g/cc
Sw	Sg	ρ_b in g/cc	Vp in m/s	Vs in m/s	σ	AI
0.1	0.9	2.133	2729.726	1563.842	0.256	5823.681
0.2	0.8	2.146	2790.886	1559.251	0.273	5989.272
0.3	0.7	2.159	2863.414	1554.701	0.291	6180.940
0.4	0.6	2.171	2950.586	1550.190	0.309	6406.228
0.5	0.5	2.184	3057.127	1545.719	0.328	6676.004
0.6	0.4	2.196	3190.132	1541.286	0.348	7006.588
0.64	0.36	2.201	3253.057	1539.523	0.356	7161.162
0.7	0.3	2.209	3360.838	1536.890	0.368	7423.795
0.8	0.2	2.221	3588.285	1532.532	0.388	7971.348
0.9	0.1	2.234	3907.908	1528.211	0.4097	8730.550
Parameter(Variable)				Symbol	Value	Unit
Pressure				P	17.237	Mpa
Water Bulk Modulus				Kw	2.507	GPa
Water Density				ρ_w	1.001	g/cc
Hydrocarbon Bulk Modulus				Khyd	0.034	Gpa
Hydrocarbon Density				ρ_{hyd}	0.118	g/cc
Sw	Sg	ρ_b in g/cc	Vp in m/s	Vs in m/s	σ	AI
0.1	0.9	2.132	2632.695	1564.632	0.227	5610.100
0.2	0.8	2.144	2690.399	1559.953	0.247	5768.429
0.3	0.7	2.157	2759.534	1555.316	0.267	5951.993
0.4	0.6	2.169	2843.596	1550.721	0.288	6169.713
0.5	0.5	2.182	2947.724	1546.165	0.310	6433.378
0.6	0.4	2.195	3079.830	1541.650	0.333	6761.131
0.7	0.3	2.208	3252.839	1537.174	0.356	7182.584
0.8	0.2	2.221	3489.582	1532.736	0.380	7750.014
0.9	0.1	2.234	3835.119	1528.337	0.406	8566.521
Parameter(Variable)				Symbol	Value	Unit
Pressure				P	13.789	Mpa
Water Bulk Modulus				Kw	2.485	GPa

Water Density				pw	0.999	g/cc
Hydrocarbon Bulk Modulus				Khyd	0.026	Gpa
Hydrocarbon Density				phyd	0.094	g/cc
Sw	Sg	pb in g/cc	Vp in m/s	Vs in m/s	σ	AI
0.1	0.9	2.128	2492.057	1565.795	0.174	5303.373
0.2	0.8	2.141	2543.325	1560.986	0.198	5445.877
0.3	0.7	2.154	2605.745	1556.221	0.223	5613.754
0.4	0.6	2.167	2683.018	1551.499	0.249	5815.464
0.5	0.5	2.181	2780.743	1546.821	0.276	6063.804
0.6	0.4	2.194	2907.864	1542.184	0.304	6379.195
0.7	0.3	2.207	3079.679	1537.588	0.334	6796.564
0.8	0.2	2.220	3324.999	1533.034	0.365	7381.629
0.9	0.1	2.233	3706.263	1528.519	0.396	8276.723
Parameter(Variable)				Symbol	Value	Unit
Pressure				P	10.342	Mpa
Water Bulk Modulus				Kw	2.4626	GPa
Water Density				pw	0.9983	g/cc
Hydrocarbon Bulk Modulus				Khyd	0.0184	Gpa
Hydrocarbon Density				phyd	0.0692	g/cc
Sw	Sg	pb in g/cc	Vp in m/s	Vs in m/s	σ	AI
0.1	0.9	2.125	2340.678	1567.000	0.094	4973.564
0.2	0.8	2.138	2383.084	1562.055	0.123	5095.775
0.3	0.7	2.152	2435.761	1557.158	0.154	5241.229
0.4	0.6	2.165	2502.416	1552.307	0.187	5418.370
0.5	0.5	2.179	2588.847	1547.499	0.222	5640.392
0.6	0.4	2.192	2704.685	1542.737	0.259	5929.209
0.7	0.3	2.206	2867.309	1538.019	0.298	6324.342
0.8	0.2	2.219	3111.956	1533.343	0.339	6905.876
0.9	0.1	2.233	3524.244	1528.710	0.384	7868.281
Parameter(Variable)				Symbol	Value	Unit
Pressure				P	6.895	Mpa
Water Bulk Modulus				Kw	2.441	GPa
Water Density				pw	0.997	g/cc
Hydrocarbon Bulk Modulus				Khyd	0.012	Gpa
Hydrocarbon Density				phyd	0.044	g/cc
Sw	Sg	pb in g/cc	Vp in m/s	Vs in m/s	σ	AI
0.1	0.9	2.122	2174.204	1568.198	-0.042	4612.781
0.2	0.8	2.135	2204.435	1563.118	-0.006	4707.362
0.3	0.7	2.149	2243.112	1558.088	0.034	4820.931
0.4	0.6	2.163	2293.580	1553.107	0.077	4961.072
0.5	0.5	2.177	2361.262	1548.172	0.123	5140.077
0.6	0.4	2.191	2455.603	1543.285	0.174	5379.354
0.7	0.3	2.204	2594.756	1538.443	0.229	5720.022
0.8	0.2	2.218	2819.014	1533.647	0.289	6253.318
0.9	0.1	2.232	3241.896	1528.895	0.357	7236.154
Calculation for Upper Gas Zone						
Input Parameters (Fixed)				Symbol	Value	Unit
Depth				D	2030-2086	M
Temperature				T	51.670	°C
Solid Material Bulk Modulus				Ks	30.000	Gpa
Solid Material Density				ps	2.772	g/cc
Logged P-wave velocity				Vpi	2850	m/s
Logged S-wave velocity				Vsi	1730	m/s
Logged Bulk Density				pbi	2.2	g/cc
Fluid Bulk Modulus at logged condition				Kfi	0.680	Gpa
Parameter(Variable)				Symbol	Value	Unit
Pressure				P	20.112	Mpa
Water Bulk Modulus				Kw	2.529	GPa
Water Density				pw	1.0025	g/cc
Hydrocarbon Bulk Modulus				Khyd	0.041	Gpa

Hydrocarbon Density				phyd	0.137	g/cc
Sw	Sg	ρb in g/cc	Vp in m/s	Vs in m/s	σ	AI
0.1	0.9	2.135	4079.303	1756.119	0.386	8709.495
0.2	0.8	2.157	4182.055	1747.284	0.394	9019.397
0.3	0.7	2.178	4301.285	1738.582	0.402	9369.639
0.4	0.6	2.199	4441.005	1730.008	0.411	9770.122
0.5	0.5	2.222	4606.738	1721.559	0.419	10234.44
0.6	0.4	2.243	4806.326	1713.234	0.427	10781.89
0.7	0.3	2.265	5051.346	1705.028	0.436	11440.87
0.8	0.2	2.286	5359.735	1696.939	0.444	12255.355
0.9	0.1	2.308	5761.096	1688.963	0.453	13297.791
Parameter(Variable)				Symbol	Value	Unit
Pressure				P	17.237	Mpa
Water Bulk Modulus				Kw	2.511	GPa
Water Density				ρw	1.001	g/cc
Hydrocarbon Bulk Modulus				Khyd	0.034	Gpa
Hydrocarbon Density				phyd	0.118	g/cc
Sw	Sg	ρb in g/cc	Vp in m/s	Vs in m/s	σ	AI
0.1	0.9	2.131	3877.3871	1757.883	0.371	8261.790
0.2	0.8	2.153	3977.849	1748.842	0.380	8563.714
0.3	0.7	2.175	4095.747	1739.939	0.389	8907.994
0.4	0.6	2.197	4235.677	1731.171	0.399	9305.888
0.5	0.5	2.219	4404.119	1722.534	0.409	9773.237
0.6	0.4	2.241	4610.553	1714.025	0.419	10333.171
0.7	0.3	2.263	4869.488	1705.641	0.430	11021.051
0.8	0.2	2.285	5204.487	1697.378	0.440	11894.201
0.9	0.1	2.307	5656.952	1689.235	0.451	13053.201
Parameter(Variable)				Symbol	Value	Unit
Pressure				P	13.789	Mpa
Water Bulk Modulus				Kw	2.488	GPa
Water Density				ρw	0.999	g/cc
Hydrocarbon Bulk Modulus				Khyd	0.027	Gpa
Hydrocarbon Density				phyd	0.094	g/cc
Sw	Sg	Pb in g/cc	Vp in m/s	Vs in m/s	σ	AI
0.1	0.9	2.125	3610.874	1760.129	0.344	7674.291
0.2	0.8	2.148	3705.482	1750.823	0.356	7959.302
0.3	0.7	2.171	3818.243	1741.664	0.369	8288.002
0.4	0.6	2.193	3954.423	1732.646	0.381	8673.177
0.5	0.5	2.216	4121.684	1723.767	0.394	9133.395
0.6	0.4	2.239	4331.667	1715.024	0.407	9696.826
0.7	0.3	2.261	4603.086	1706.412	0.420	10408.69
0.8	0.2	2.284	4968.359	1697.928	0.434	11347.21
0.9	0.1	2.306	5489.815	1689.570	0.448	12662.52
Parameter(Variable)				Symbol	Value	Unit
Pressure				P	10.342	Mpa
Water Bulk Modulus				Kw	2.466	GPa
Water Density				ρw	0.995	g/cc
Hydrocarbon Bulk Modulus				Khyd	0.019	Gpa
Hydrocarbon Density				phyd	0.069	g/cc
Sw	Sg	ρb in g/cc	Vp in m/s	Vs in m/s	σ	AI
0.1	0.9	2.119	3307.406	1762.468	0.302	7010.674
0.2	0.8	2.143	3391.417	1752.885	0.318	7267.569
0.3	0.7	2.167	3493.488	1743.457	0.334	7567.488
0.4	0.6	2.189	3619.404	1734.179	0.351	7924.359
0.5	0.5	2.213	3777.875	1725.048	0.368	8359.115
0.6	0.4	2.236	3982.724	1716.059	0.386	8904.934
0.7	0.3	2.259	4257.467	1707.209	0.404	9618.172
0.8	0.2	2.282	4646.112	1698.496	0.423	10604.146
0.9	0.1	2.306	5243.464	1689.914	0.442	12089.383
Parameter(Variable)				Symbol	Value	Unit
Pressure				P	6.895	Mpa

Water Bulk Modulus				Kw	2.444	GPa
Water Density				ρw	0.997	g/cc
Hydrocarbon Bulk Modulus				Khyd	0.012	Gpa
Hydrocarbon Density				ρhyd	0.044	g/cc
Sw	Sg	ρb in g/cc	Vp in m/s	Vs in m/s	σ	AI
0.1	0.9	2.114	2949.535	1764.779	0.221	6235.738
0.2	0.8	2.138	3015.529	1754.921	0.244	6447.081
0.3	0.7	2.1625	3097.940	1745.227	0.268	6697.058
0.4	0.6	2.186	3202.626	1735.692	0.292	6999.643
0.5	0.5	2.209	3338.768	1726.311	0.317	7376.716
0.6	0.4	2.233	3521.704	1717.081	0.344	7864.777
0.7	0.3	2.257	3779.366	1707.997	0.372	8530.210
0.8	0.2	2.281	4169.341	1699.056	0.400	9509.705
0.9	0.1	2.305	4836.157	1690.254	0.430	11145.805
Calculation for New Gas Zone I						
Input Parameters (Fixed)				Symbol	Value	Unit
Depth				D	2148-2154	M
Temperature				T	55.56	°C
Solid Material Bulk Modulus				Ks	30	Gpa
Solid Material Density				ρs	2.75	g/cc
Logged P-wave velocity				Vpi	2180	m/s
Logged S-wave velocity				Vsi	1320	m/s
Logged Bulk Density				ρbi	2.2	g/cc
Fluid Bulk Modulus at logged condition				Kfi	0.766	Gpa
Parameter(Variable)				Symbol	Value	Unit
Pressure				P	21.284	Mpa
Water Bulk Modulus				Kw	2.548	GPa
Water Density				Pw	1.002	g/cc
Hydrocarbon Bulk Modulus				Khyd	0.044	Gpa
Hydrocarbon Density				Phyd	0.141	g/cc
Sw	Sg	ρb in g/cc	Vp in m/s	Vs in m/s	σ	AI
0.1	0.9	2.124	2838.477	1343.295	0.356	6029.941
0.2	0.8	2.146	2915.875	1336.598	0.367	6256.589
0.3	0.7	2.167	3007.793	1330.001	0.378	6518.003
0.4	0.6	2.188	3118.426	1323.500	0.390	6824.298
0.43	0.57	2.195	3156.109	1321.568	0.394	6926.969
0.5	0.5	2.210	3253.869	1317.094	0.402	7190.139
0.6	0.4	2.231	3423.369	1310.779	0.414	7637.742
0.7	0.3	2.252	3641.761	1304.555	0.426	8202.703
0.8	0.2	2.274	3934.676	1298.419	0.439	8946.434
0.9	0.1	2.295	4351.228	1292.368	0.452	9986.421
Parameter(Variable)				Symbol	Value	Unit
Pressure				P	17.237	Mpa
Water Bulk Modulus				Kw	2.521	GPa
Water Density				ρw	0.999	g/cc
Hydrocarbon Bulk Modulus				Khyd	0.034	Gpa
Hydrocarbon Density				ρhyd	0.115	g/cc
Sw	Sg	ρb in g/cc	Vp in m/s	Vs in m/s	σ	AI
0.1	0.9	2.119	2641.934	1345.127	0.325	5597.142
0.2	0.8	2.141	2712.832	1338.217	0.339	5806.845
0.3	0.7	2.162	2798.289	1331.413	0.354	6051.141
0.4	0.6	2.184	2902.865	1324.712	0.368	6340.949
0.5	0.5	2.206	3033.368	1318.111	0.384	6692.550
0.6	0.4	2.228	3200.497	1311.608	0.399	7131.485
0.7	0.3	2.250	3422.209	1305.199	0.415	7700.573
0.8	0.2	2.272	3731.514	1298.885	0.431	8478.406
0.9	0.1	2.294	4197.637	1292.661	0.448	9629.556
Parameter(Variable)				Symbol	Value	Unit
Pressure				P	13.789	Mpa
Water Bulk Modulus				Kw	2.499	GPa
Water Density				ρw	0.999	g/cc

Hydrocarbon Bulk Modulus				Khyd	0.026	Gpa
Hydrocarbon Density				phyd	0.092	g/cc
Sw	Sg	pb in g/cc	Vp in m/s	Vs in m/s	σ	AI
0.1	0.9	2.113	2463.063	1346.805	0.287	5205.191
0.2	0.8	2.136	2526.102	1339.697	0.304	5395.206
0.3	0.7	2.158	2603.235	1332.701	0.322	5618.476
0.4	0.6	2.181	2699.190	1325.813	0.341	5886.261
0.5	0.5	2.203	2821.203	1319.031	0.360	6215.773
0.6	0.4	2.226	2981.008	1312.352	0.379	6634.884
0.7	0.3	2.248	3199.142	1305.773	0.400	7192.316
0.8	0.2	2.271	3515.632	1299.292	0.421	7982.895
0.9	0.1	2.293	4022.309	1292.907	0.442	9223.836
Parameter(Variable)				Symbol	Value	Unit
Pressure				P	10.342	Mpa
Water Bulk Modulus				Kw	2.476	GPa
Water Density				ρ_w	0.997	g/cc
Hydrocarbon Bulk Modulus				Khyd	0.018	Gpa
Hydrocarbon Density				phyd	0.068	g/cc
Sw	Sg	pb in g/cc	Vp in m/s	Vs in m/s	σ	AI
0.1	0.9	2.1082	2268.428	1348.548	0.227	4781.487
0.2	0.8	2.131	2320.761	1341.234	0.249	4945.292
0.3	0.7	2.154	2386.048	1334.037	0.273	5139.416
0.4	0.6	2.177	2468.957	1326.956	0.297	5374.911
0.5	0.5	2.200	2576.825	1319.986	0.322	5669.138
0.6	0.4	2.223	2721.968	1313.124	0.348	6051.205
0.7	0.3	2.246	2926.963	1306.369	0.376	6574.401
0.8	0.2	2.269	3238.837	1299.717	0.404	7349.576
0.9	0.1	2.292	3777.669	1293.165	0.434	8659.377
Parameter(Variable)				Symbol	Value	Unit
Pressure				P	6.895	Mpa
Water Bulk Modulus				Kw	2.454	GPa
Water Density				ρ_w	0.996	g/cc
Hydrocarbon Bulk Modulus				Khyd	0.012	Gpa
Hydrocarbon Density				phyd	0.044	g/cc
Sw	Sg	pb in g/cc	Vp in m/s	Vs in m/s	σ	AI
0.1	0.9	2.102	2051.069	1350.284	0.118	4312.218
0.2	0.8	2.126	2088.630	1342.765	0.148	4440.506
0.3	0.7	2.149	2136.939	1335.369	0.179	4593.667
0.4	0.6	2.173	2200.180	1328.095	0.213	4781.566
0.5	0.5	2.197	2285.151	1320.939	0.249	5020.188
0.6	0.4	2.220	2403.726	1313.897	0.287	5337.438
0.7	0.3	2.244	2578.881	1306.966	0.327	5787.259
0.8	0.2	2.268	2862.415	1300.144	0.370	6491.127
0.9	0.1	2.291	3405.681	1293.428	0.416	7803.511

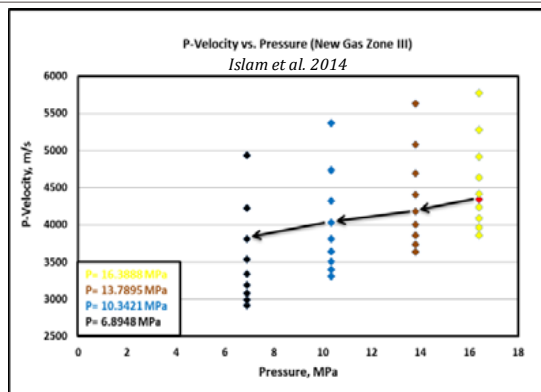
Table 8: Calculated fluid and rock properties from Gassmann-Biot Model (for varying saturation and pressure).

of water saturation effects on fluid properties by increasing the fluid density, modulus and acoustic velocity among the all gas sand layers of the Fenchuganj Gas Field. The compressibility of fluid declines as the water in fluid rises. Similarly, due to temperature rises, the velocity and density of the fluid fall. The cross plots using the Batzle and Wang model on densities and moduli allows to predict the fluid properties as the reservoir is produced and shows the effect on the reservoir as water saturation rises and gas saturation drops. The modify in P-wave and S- wave velocity, bulk density, acoustic impedance, Poisson's ratio, and bulk modulus were predicted using the Batzle and Wang and Gassmann-Biot model which show that the reservoir changes from irreducible water saturation conditions in residual gas conditions which provide an avenue to calculate values at reservoir conditions from logging conditions. Coupling with the Batzle and Wang, Gassmann-Biot, the AVO models can be used to determine expected

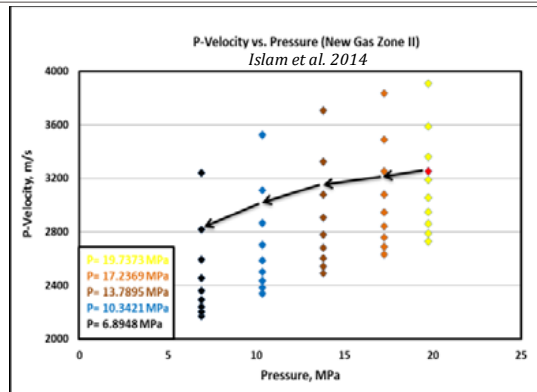
seismic responses throughout the production path of the reservoir and coincide with previous results [17]. In case of the Fenchuganj Gas Field, it is shown that an AVO response is presented as a result of the fluid and rock properties and also show that the reservoir is pressure decreases due to increasing the gas production. The AVO modeling for fluid property investigation will help in determining the usefulness of time lapse seismic, predicting AVO and amplitude response, and making decision on forecasting and production for the reservoir.

Acknowledgement

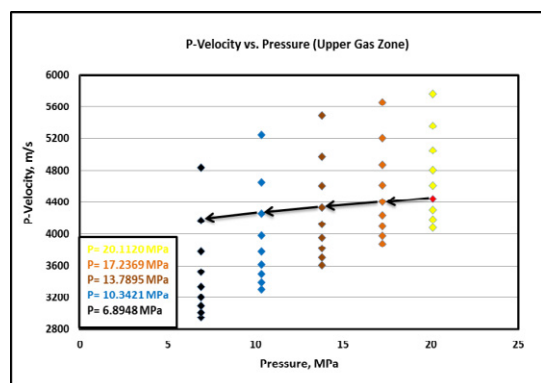
The authors are grateful to BAPEX authority, especially Geological and Geophysical Division for allowing collecting the necessary data and use their software for this work. The first author is also grateful to Mr. Md. Shofiqul Islam, Geology Division (BAPEX) and Mr. Pulok Kanti Deb, Department of Petroleum and Mining Engineering, Shahjalal University for their help and suggestions to improve this work.



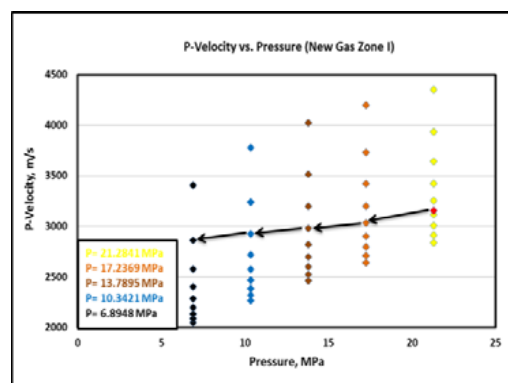
a.



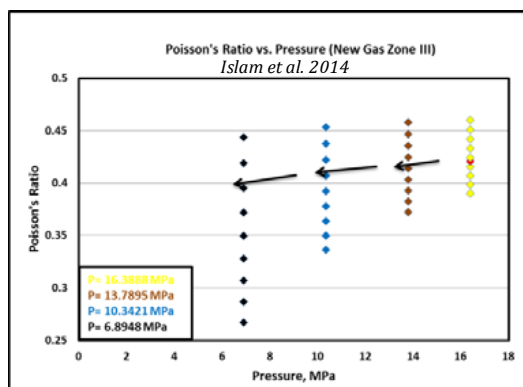
b.



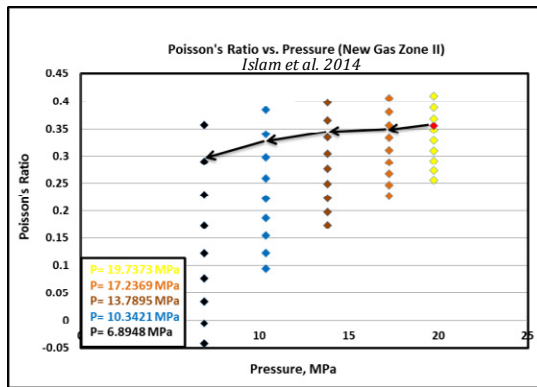
c.



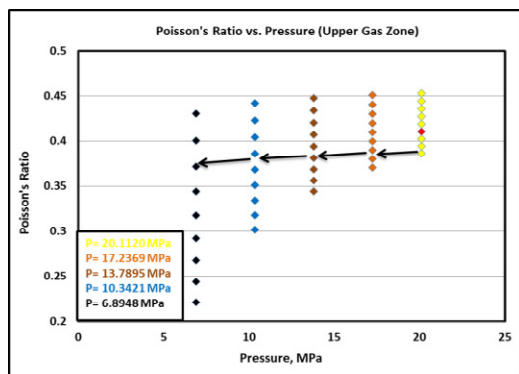
d.



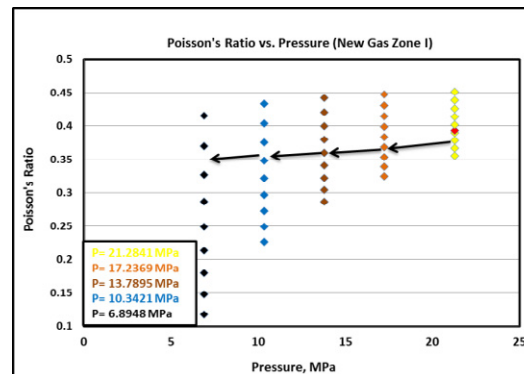
e.



f.



g.



h.

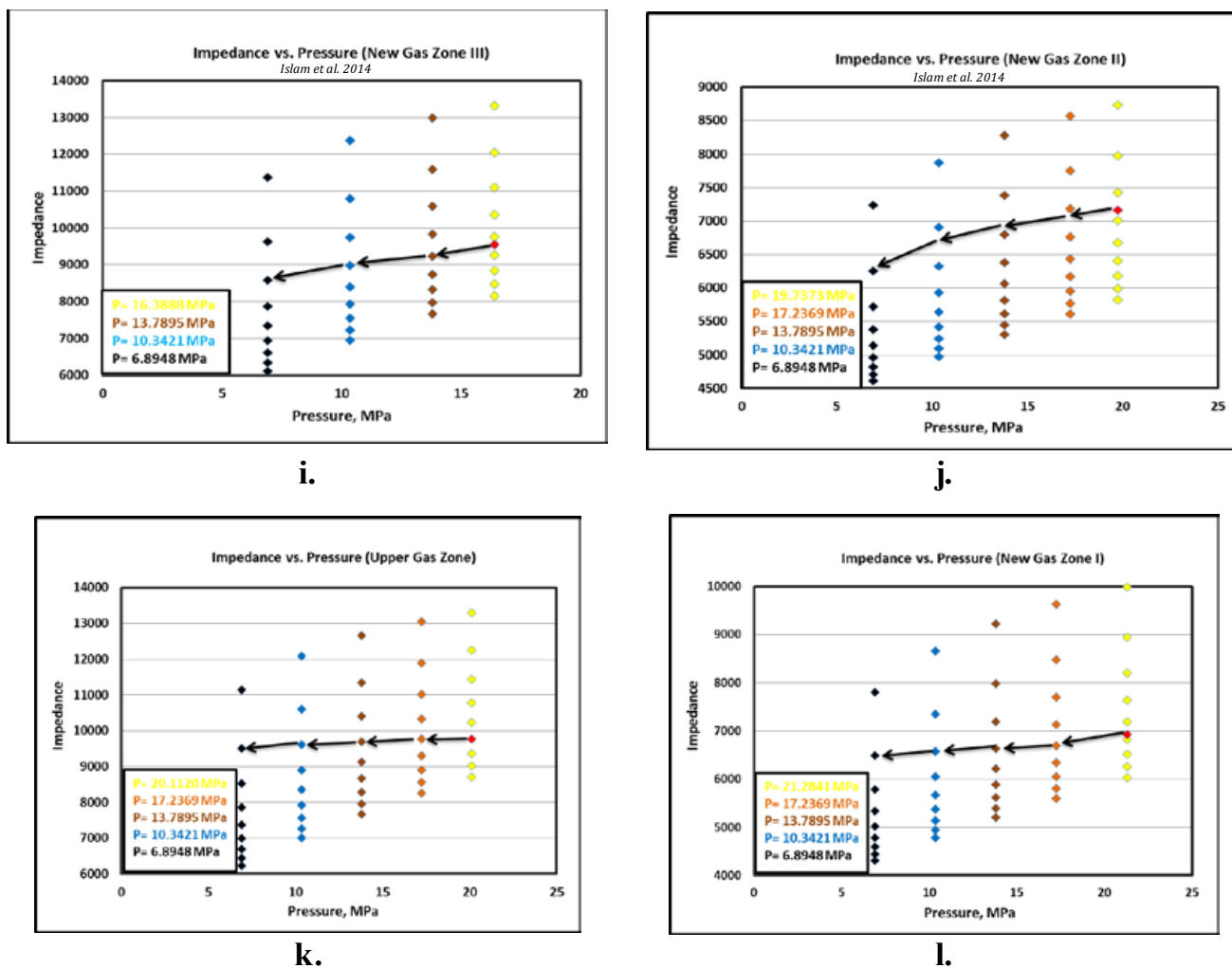
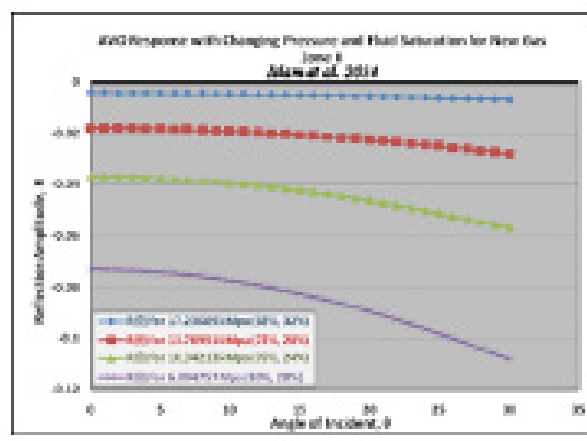
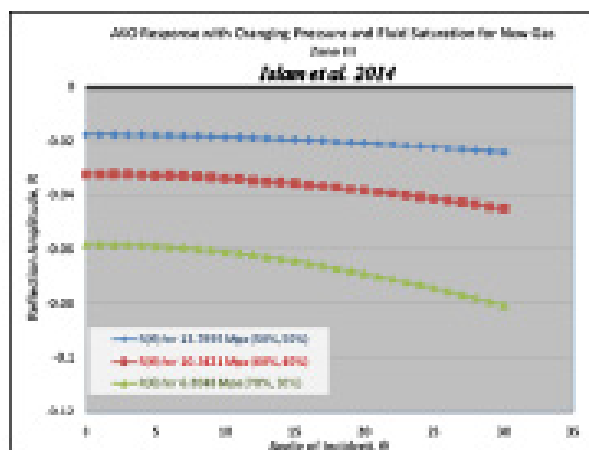


Figure 7: (a-d) P-wave velocity versus pressure shows how the velocity changes as the pressure and saturation in the reservoir changes; (e-h) The Poisson's ratio versus pressure shows how the velocity changes as the pressure and saturation in the reservoir changes; and (i-j) Acoustic impedance versus pressure show how the Poisson's ratio changes as the pressure and saturation in the reservoir changes.



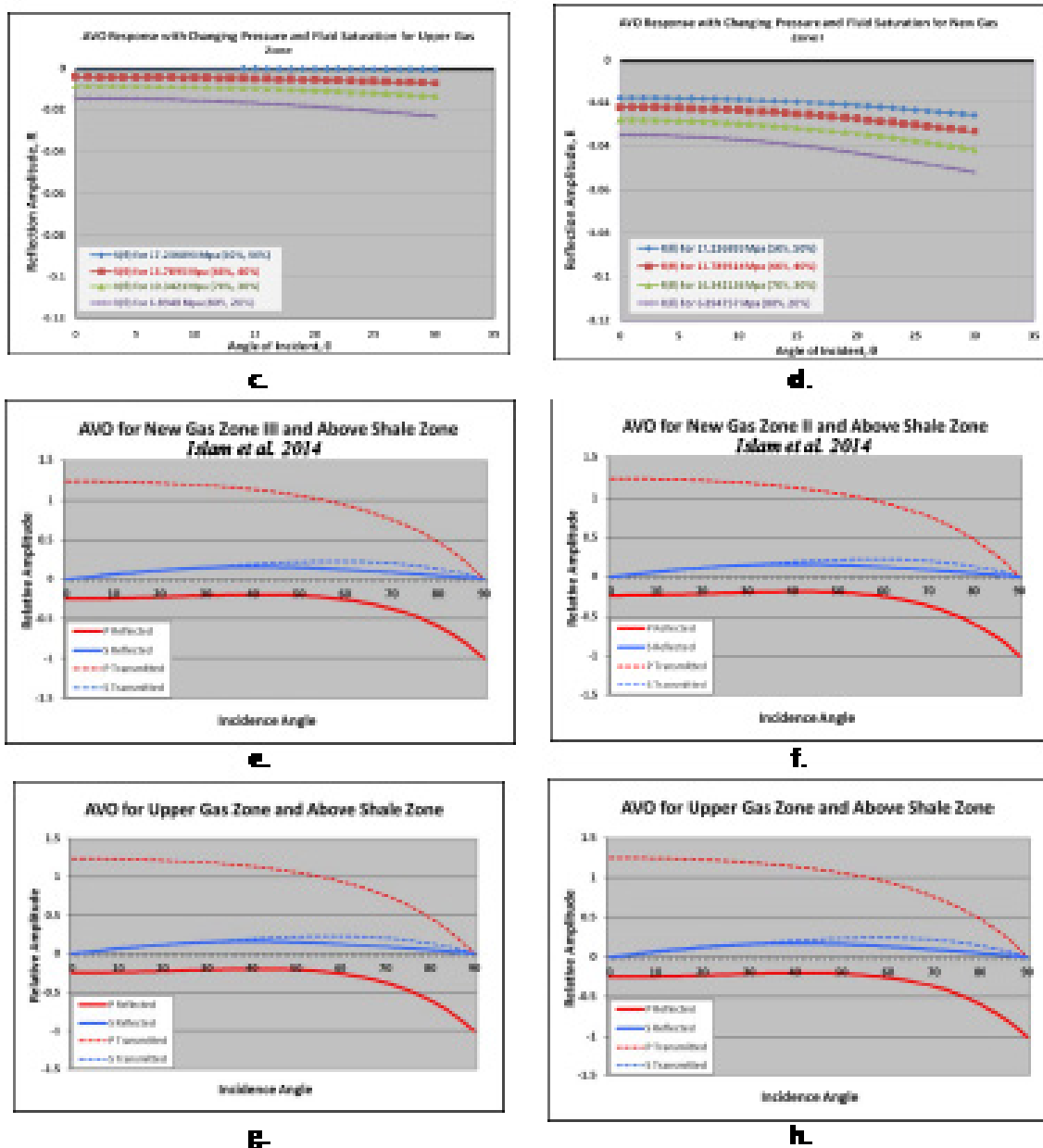


Figure 8: Reflection amplitude versus offset shows the AVO between a definite pressure-saturation condition and reservoir condition for a) New Gas Zone III, b) New Gas Zone II, c) Upper Gas Zone and d) New Gas Zone I. Reflection amplitude versus offset shows the AVO between e) New Gas Zone III and above shale zone, b) New Gas Zone II and above shale zone, c) Upper Gas Zone and above shale zone, and h) New Gas Zone I and above shale zone.

Above Shale Zone/ Gas Zone	P-Velocity (Vp)		S-Velocity (Vs)		Bulk Density (ρ_b) g/cm ³
	m/sec	ft/sec	m/sec	ft/sec	
Shale Zone Above New gas Zone III	4000	13123	2116	6942	2.40
Shale Zone Above New gas Zone II	3800	12467	2011	6598	2.40
Shale Zone Upper gas Zone	4300	14107	2275	7464	2.40
Shale Zone New gas Zone I	3300	10826	1746	5728	2.40
New gas Zone III	2650	8694	1606	5269	2.20
New gas Zone II	2540	8333	1540	5053	2.20
Upper gas Zone	2850	9350	1730	5676	2.20
New gas Zone I	2180	7152	1320	4330	2.20

Table 9: The inputs for Shale zones above gas layer and Gas zones for determining AVO.

References

1. Zoeppritz K (1919) Erdbebenwellen, VIII B, On the reflection and propagation of seismic waves. *Gottinger Nachrichten* 1: 66-84.
2. Gassmann F (1951) Elastic waves through a packing of spheres. *Geophysics* 16: 673-685.
3. Biot MA (1956) Theory of propagation of elastic waves in a fluid-saturated porous solid. *J Acoustic Soc America*, 28: 168-191.
4. Kuster GT, Toksöz MN (1974) Velocity and attenuation of seismic waves in two-phase media: Part I. theoretical formulations. *Geophysics* 39: 587-606.
5. O'Connell R, Budiansky B (1974) Seismic velocities in dry and saturated crack solids. *J Geophys Res* 79: 5412-5426.
6. Rutherford SR, Williams RH (1989) Amplitude-versus-offset variations in gas sands. *Geophysics* 54: 680-688.
7. Mavko G, Jizba D (1991) Estimating grain-scale fluid effects on velocity dispersion in rocks. *Geophysics* 56: 1940-1949.
8. Batzle M, Wang Z (1992) Seismic properties of pore fluids. *Geophysics* 57: 1396-1408.
9. Sheriff RE (1991) *Encyclopedic Dictionary of Exploration Geophysics*. (3rd Edn) SEG Geophysical References Series 1, Tulsa, USA.
10. Castagna JP, Swan HW (1997) Principles of AVO cross plotting. *The Leading Edge* 16: 337-342.
11. Bulloch TE (1999) The investigation of fluid properties and seismic attributes for reservoir characterization. M.Sc thesis for Geological Engineering, Michigan Technological University, USA.
12. <http://www.glossary.oilfield.slb.com/en/Terms.aspx?LookIn=term%20name&filter=amplitude%20variation%20with%20offset>
13. Annual Report (2010) Bangladesh Petroleum Exploration and Production Company Limited (BAPEX), Bangladesh.
14. Geological Survey Bulletin (2001) U.S Geological Survey -Petrobranga cooperative assessment of undiscovered natural gas resources of Bangladesh. U.S. 2208-A: 119.
15. Evans P (1964) The tectonic framework of Assam. *J Geol Soc Ind* 5: 80-96.
16. Hiller K, Elahi M (1984) Structural development and hydrocarbon entrapment in the Surma Basin, Bangladesh (northwest Indo-Burman fold belt). Singapore Fifth Offshore Southwest Conference, Singapore.
17. Islam S M A, Islam M S, Hossain M M (2014) Investigation of fluid properties and their effect on seismic response. A case study of Fenchuganj Gas Field, Surma Basin, Bangladesh. *Int J Oil Gas Coal Engg* 2: 36-54.
18. Hilterman F (1989) Is AVO the seismic signature of rock properties?. 59th Ann Internat Mtg, Soc. Expl. Geophys. Expanded Abstracts.
19. Knigh R, Nolen-Hoeksema RA (1990) laboratory study of the dependence of elastic wave velocities on porescale fluid distribution. *Geophys Res Lett* 17: 1529-1532.
20. Liu Zhupin WU, Xiaowei Chu Zehan (1994) Laboratory study of acoustic parameters of rock. *Chinese J Geophys* 37: 659-666.
21. Gregory AR (1976) Fluid saturation on dynamic elastic properties of sedimentary rocks. *Geophysics* 41: 895-921.
22. Aki K, Richards PG (1980) *Quantitative seismology: Theory and methods*. W.H.Freeman and Co.
23. Shuey RT (1985) A simplification of the Zoeppritz equations. *Geophysics* 50: 609-614.